Relative Sea Level Change Along Quinault Indian Reservation Marine Coastlines

William E. Schlosser

2013

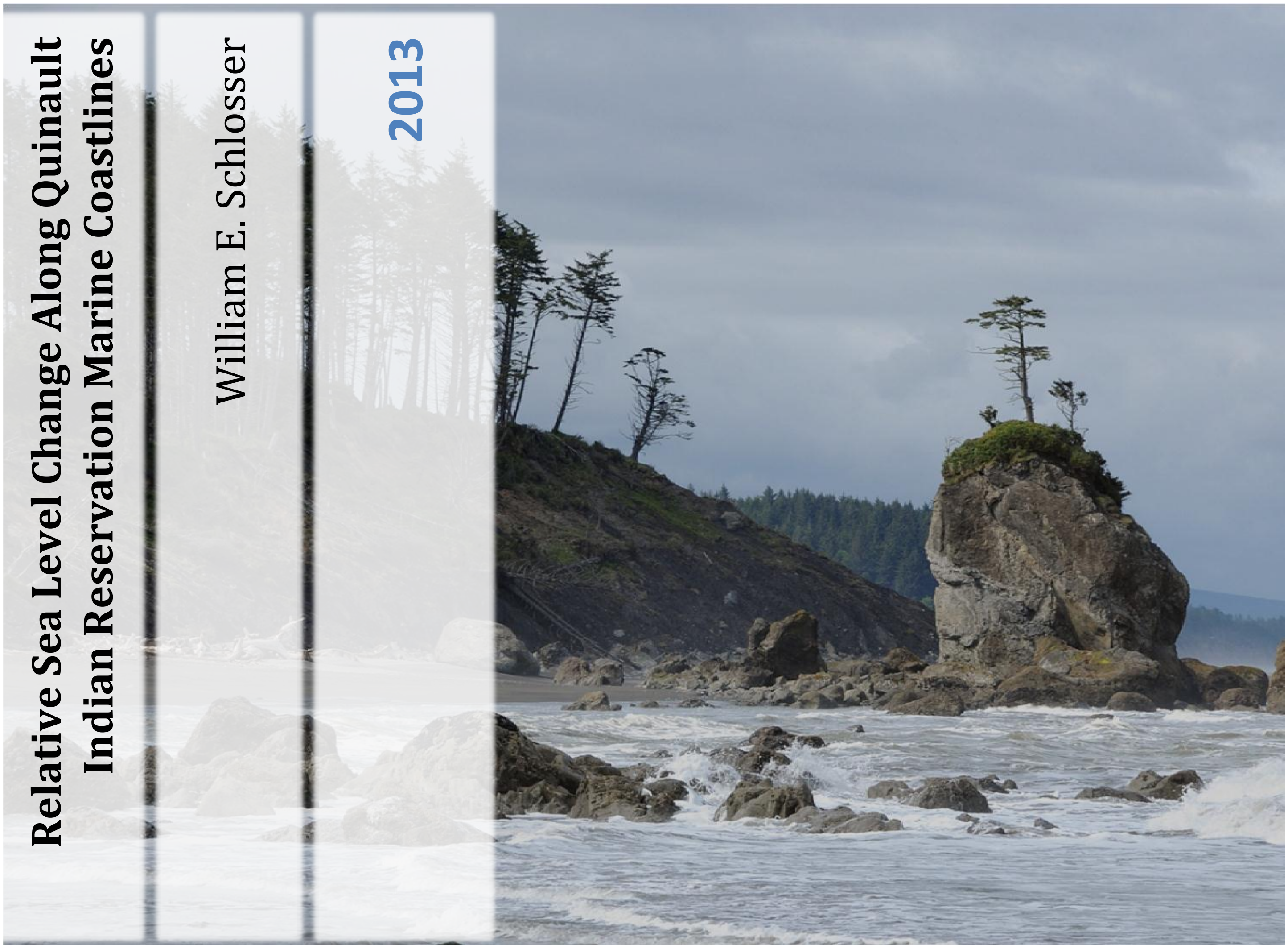

Relative Sea Level Change is observed through the combined effects of global sea level change with local factors such as vertical land deformation (e.g., tectonic movement, isostatic rebound) and seasonal sea level ocean elevation changes due to atmospheric circulation effects. Available projections of these factors for the coastal waters of the Quinault Indian Reservation are estimated from the results of primary and secondary research and combined with marine shoreline field observations to provide estimates of local Relative Sea Level Change through 2100.

Kamiak Ridge, LLC
1515 NW Kenny Dr
Pullman WA 99163
360-637-6798
Schlosser@Resource-Analysis.com
www.Resource-Analysis.com

This **Relative Sea Level Change along the Quinault Indian Reservation Coastlines** Document, is completed in the fulfillment of a Contract entered into by the Quinault Indian Nation and Kamiak Ridge, LLC

Project Administration provided by

Michael Cardwell, Director
Division of Community Services
Quinault Indian Nation
PO Box 189
Taholah, WA 98587

Planning services, analysis, and document authorship provided by

William E. Schlosser, Ph.D.
Kamiak Ridge, LLC
1515 NW Kenny Dr.
Pullman WA 99163
www.Resource-Analysis.com

This planning effort has been completed with the consultation by a Planning Committee comprised of representatives of administrative Divisions of the Quinault Indian Nation, including the Division of Community Services, Division of Natural Resources, Division of Centralized Communications, and planning consultants from Kamiak Ridge, LLC.

Chapter 0. Table of Contents

0.1. List of Tables

0.2. List of Figures

0.3. Acronyms Used

Chapter 1. Introduction & Conveyance

1.1. Introduction

The Quinault Indian Reservation is located along the central ocean coastline of the state of Washington (Figure 1). A study of the relative sea level change along the Quinault Indian Reservation marine coastlines was requested by the Quinault Indian Nation Business Council to address the significant effects of global climate change on the Quinault Indian Reservation's marine shorelines. This document addresses specific expected changes and their influence in the area taking into account the factors of global climate change, rising sea level expectations, tectonic rebound following the retreat of glaciers along this coastline, geologic parent material soil types, and other factors. This analysis identifies expected areas of significant marine shoreline changes in the context of these impacts during the coming century.

This assessment is a part of an ongoing effort by the Quinault Indian Nation to address the Quinault Indian Reservation's shorelines in three segments:

1. Marine Shorelines
2. River Shorelines
3. Lake Shorelines

Although these three classifications of shorelines are highly interrelated, they are addressed separately through unified planning efforts. This report launches into all three components of the Quinault Indian Nation's Shoreline Management Planning Framework, but relates primarily to the first component; Marine Shorelines.

The goal of this Relative Sea Level Change (RSLC) document is to consider the influence of recent scientific research to provide a sound framework to address issues of shoreline management within the Quinault Indian Reservation. This document is a predecessor to the QIN Shoreline Management Plan and serves to develop many of the findings of significance that affect each of the components of the planning effort.

1.1. Authorship

Development of the Relative Sea Level Change Assessment along the Quinault Indian Reservation's Marine Coastline was completed by Kamiak Ridge, LLC. Project Management duties and Lead Authorship of this plan have been provided by William E. Schlosser, Ph.D., a Regional Planner and Environmental Scientist.

The undersigned do hereby attest and affirm that the Relative Sea Level Change Assessment along the Quinault Indian Reservation's Marine Coastline was completed using information available at the time of its writing. Furthermore, analysis techniques were implemented as appropriate to provide a clear and reasonable assessment of Relative Sea Level Change along the marine coastlines of the Quinault Indian Reservation.

Kamiak Ridge, LLC

By: William E. Schlosser, Ph.D. Kamiak Ridge, LLC Environmental Scientist & Regional Planner Lead Author and Project Mananger	January 31, 2013 Date
By: Birgit R. Schlosser, B.A. Kamiak Ridge, LLC Co-Owner & Planning Specialist	January 31, 2013 Date

Figure 1. Quinault Indian Reservation, location map.

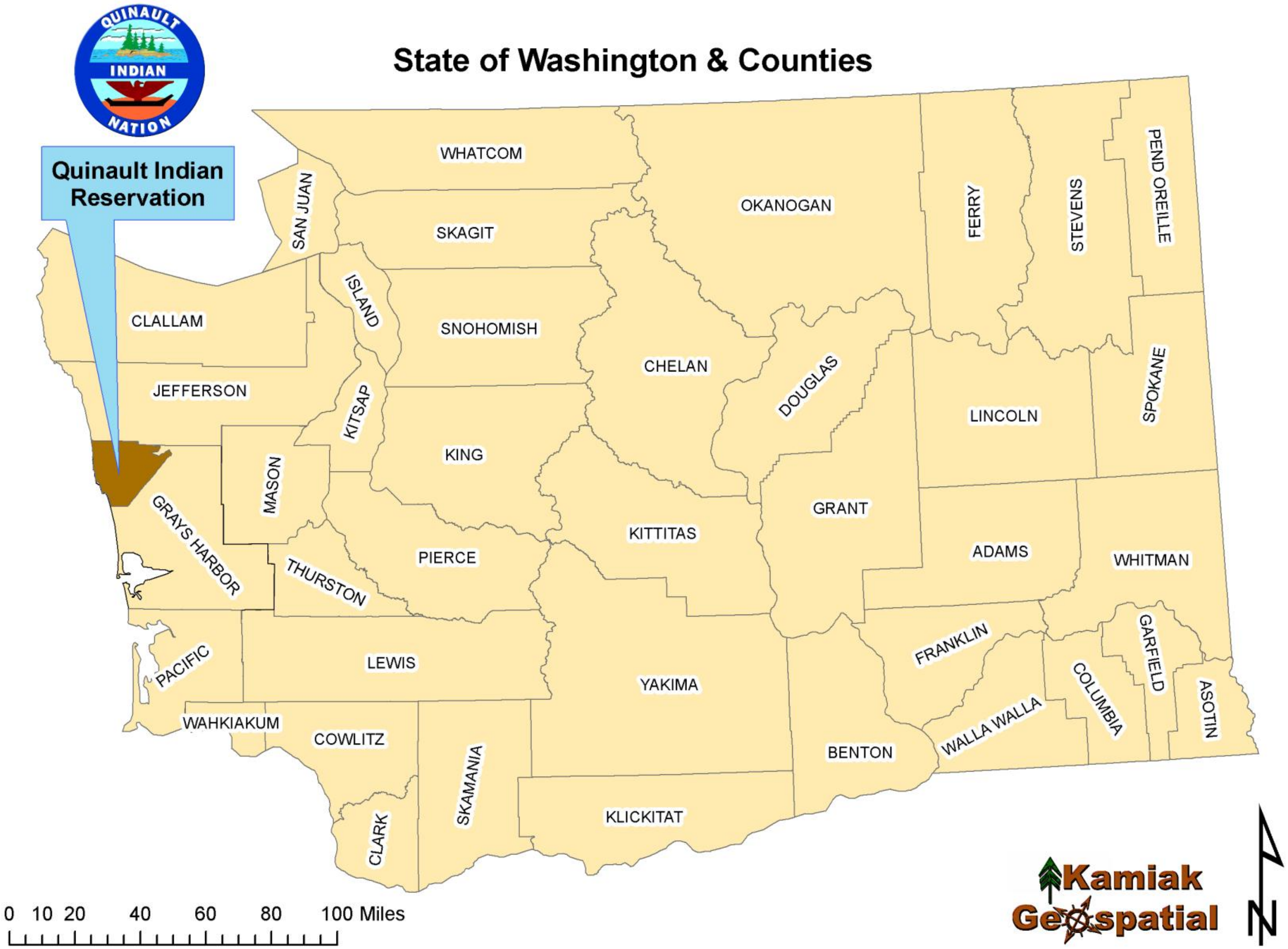

Chapter 2. Earth Processes within the QIR

The information presented in this chapter is based greatly on written reports and geospatial data provided by the Washington State Department of Natural Resources, Division of Geology and Earth Resources; the Cascadia Region Earthquake Workgroup (CREW) (CREW 2005); the U.S. Geological Survey (USGS); Geologists Weldon Rau (Rau 1973), Dan Orange, and Kathy Campbell (Orange and Campbell 1996); and is supported by site visits and investigations conducted by Kamiak Ridge staff. This report guides the reader through the integration of these features, to build an understanding of the past while we look into the next century and make predictions about how events may develop.

2.1. The Formation of Quinault Ocean Shoreline Rocks

Within the Quinault ocean shorelines and near-shore areas, the land formations seen today, have been building since at least the Eocene Epoch[1] (about 50 million years ago) with the mixing of offshore sedimentary rocks with basalt (igneous rocks) that in time had been metamorphically reshaped, crumbled, and pushed to rest at Point Grenville (Figure 2). During the Miocene Epoch (about 7 to 22 million years ago), the Hoh Rock Formations were formed offshore from siltstone, sandstone, and conglomerates (Figure 2). Those massive formation materials transformed by tectonic processes had eventually led to the formation of the Olympic Peninsula where they have provided the foundation of much of the northern landscapes. As the Pliocene Epoch unfolded (1.5 to 7 million years ago), the Quinault Formation was formed in deep sea floor environments from consolidated, stratified, and then tilted sedimentary rocks. These sedimentary rocks are younger in geologic age than the Hoh Assemblage rocks and the basaltic remnants scattered under the Quinault Formation. Sometimes, the combined effect of tectonic forces has resulted in tilting these formations to the point that even the basalt layers of the Miocene Epoch ended up overturned to be found on top of Quinault Formation structures.

All of these geologic structures have been formed during the Cenozoic Era (within the last 65 million years), the most recent era of earth history reaching through time as far back as over 4.5 billion years (Figure 2). The "geologically recent" events include the creation, advancement, and retreat of glacial periods. Overlying the bedrock all along this coast deposits of sand and gravel are found that had been brought by streams from melting glaciers during the Pleistocene Epoch some 17 to 70 thousand years ago (Rau 1973). The changes to this landscape have led to the expansion of dense forests, meandering mighty rivers, the movement of salmon into those rivers, and the flourish of human habitation in the form of the Quinault people and other indigenous peoples of this region.

Weldon Rau (Geology of the Washington Coast; Point Grenville and the Hoh River 1973) completed an insightful and extensive assessment of the marine coastline lithology. This assessment has been updated on several key points, but the basis of that assessment provides extensive fundamental illustrations of the status of this coastline. One of the most substantial updates to the work of Rau comes from Orange and Campbell (1996) providing a well-considered description of the QIR's marine shoreline geologic processes.

The highly variable QIR ocean coastline had been formed as a result of geological processes that eventually defined currently existing combination of parent materials, soils, and rock

[1] The tern Epoch refers to a geologic period during which a geologic series is formed covering the formation and development of the Earth, from about 4.5 billion years ago to today.

formations in the area. South of Point Grenville, the CRLC (see Section 2.3) dominates the shoreline with high-energy and gentle off-shore slopes, all capped with a thick contribution of sands and silt materials. The bedrock of Point Grenville is basalt in origin which had been solidified on the seafloor some 45 to 50 million years ago. Northward, along the coastline bedrock of the cliff gently dipping sandstone and siltstone beds of the Quinault Formation are observed. The sandstone and conglomerate rocks of Cape Elizabeth, also of the Quinault Formation, form many high cliffs, including Cape Elizabeth, Pratt Cliff, and Tunnel Island.

A major collection of geologic materials along the coastline is the Hoh Rock Assemblage. It is structurally very weak and highly susceptible to erosion. For example, north of Cape Elizabeth, where the formation is exposed at shoreline cliffs, it has slumped and eroded extensively as a result of the nature of clay which expands when wetted by ocean waves and precipitation. This rock type extends along the shoreline and is intermittently found starting from Point Grenville and extending as far as the Hoh River. It may be described as a highly folded, steeply tilted sandstone and siltstone sequence. Although broken in places by faulting, it generally constitutes a coherent sequence of sandstone and siltstone strata.

Another group of rock formation called a "Tectonic Mélange" presents a chaotic mixture of siltstone, sandstone, conglomerate, and volcanic material that are blended into a viscous mix of materials, gradually extruded by deep-mantle pressures through the overtopping materials of a piercement structure. A piercement structure appears to be a dome or anticlinal fold[2] exposed to pressure, in which a mobile plastic core has ruptured through the more brittle overlying rock. These are also known as diapir (e.g., Duck Creek Diapir), piercement dome, and piercing fold. Such rocks are exposed in a number of places along the QIR coast and are easily observed in the cliffs for a distance of about 2 miles immediately south of Raft River in the Hogsback area.

Resistant boulder chunks within this assemblage of rock are often formed by volcanic processes and are extremely large. As the softer Hoh Rock Assemblage matrix had been gradually eroded away by wave action and rains, these resistant boulders were left behind. Big and Little Hogsback, Willoughby Rock, Split Rock and the large boulders in the Hogsback vicinity had been formed in this way. The coastal rock formations between Point Grenville and Queets are mostly basalt in origin with a few interbeds[3] of ocean siltstone such as those seen near Point Grenville. Microfossils contained in these interbeds indicate that they were formed some 45 to 50 million years ago during middle Eocene time (Figure 2). The basaltic materials were formed as a result of submarine lava flows that had been vented from along the Juan de Fuca plate as it passed the CSZ and then broken off from the plate onto the mélange of sea-mud, sands, silts, and other materials (Figure 9) (Rau 1973).

[2] A shaped deformation in a geologic structure inclining downward on both sides from a median line or axis, such as a fold of rock strata.

[3] A layer of sediments or rock that extends under a large area and has a distinct set of characteristics that distinguish it from other layers below and above it.

Figure 2. Geologic Chronology along QIR Marine Coastline (reproduced from (Rau 1973)).

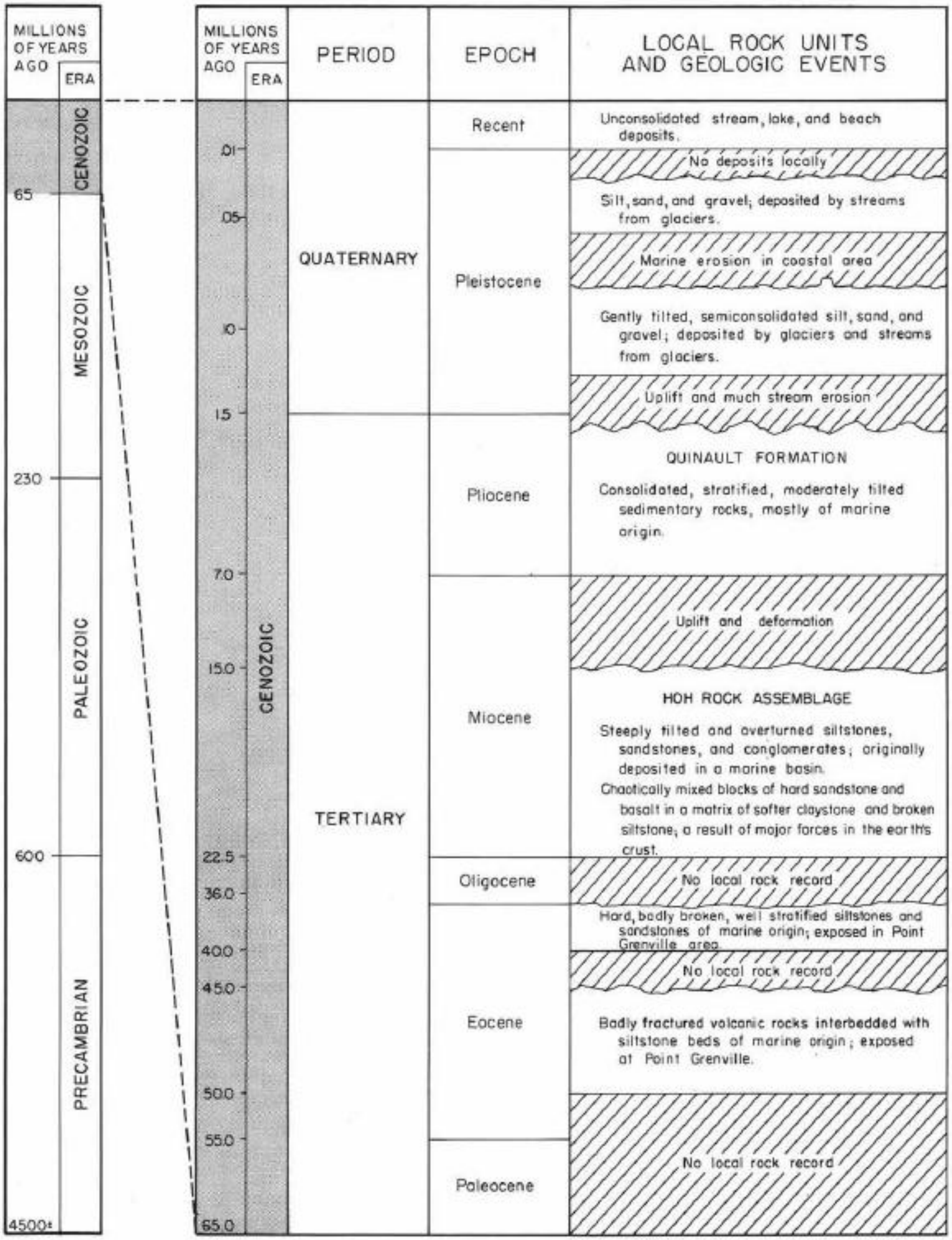

2.2. Plates, Faults, Earthquakes, and Subduction

The crust or surface of our planet is broken into large, irregularly shaped pieces called tectonic plates. The plates respond to movements in the earth's center to slide past each other (transform plate boundaries), pull apart (divergent plate boundaries), or push together (convergent plate boundaries). Transform boundaries result in lateral movement of the plates. Divergent plates result in sea-floor spreading. Convergent plates result in a) mountain building, in the case of two continental plates meeting or b) subduction zones formed when oceanic and continental plates meet. The oceanic plate is denser and is therefore forced underneath the lighter continental plate at the convergent plate boundary. At a certain depth in the planetary asthenosphere (Figure 3), the submerged oceanic plate begins to melt. The melted basaltic crust, known as magma, causes asthenosphere pressures to rise and results in fluid magma uplift into the continental crust forming stratovolcanoes.

Stratovolcanoes are common above subduction zones. They are formed as magma rises in response to mantle pressure changes. The lithosphere materials, when pushed down into the asthenosphere, are melted into magma. Water trapped both in hydrated minerals and in the porous basalt rock of the oceanic crust is released into magma of the asthenosphere (Figure 3) (Kious and Tilling 1999). As the oceanic plate descends, the release of water occurs at specific pressures and temperatures for each mineral. The water freed from the rock lowers the melting point of the overlying continental plate, which then undergoes partial melting and rises due to its lighter density relative to the surrounding rock. When the magma nears the surface of the continent, it pools into a magma chamber under or within the volcano. When a volume of accumulated magma and gas has achieved a critical point, the blockage within the volcanic cone is released, leading to a sudden explosive eruption (Kious and Tilling 1999).

Figure 3. A thin semi-fluid layer of the earth's mantle is the Asthenoshpere, overtopped by the rigid Lithosphere (ArchitectJaved.com 2012).

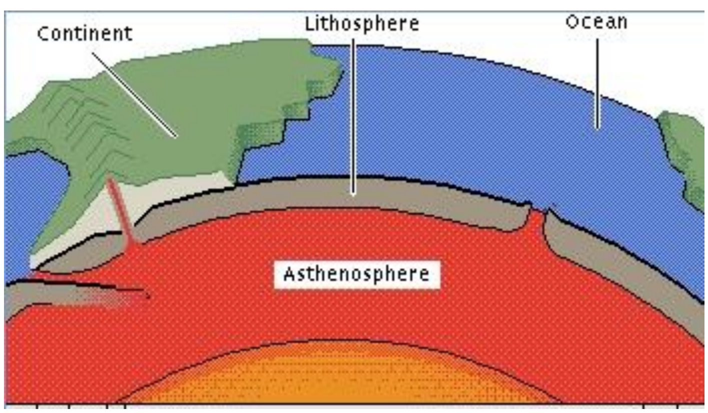

As the oceanic plate moves through the Subduction zone, the oceanic sediments are scraped off its surface. These sediments are accreted, deformed, and uplifted during the shift. This wedge of sedimentary materials is pushed up to the level of the land surface of the Olympic Peninsula and then may be eroded and transported back to the ocean to be recycled once again (Hellwig 2010) (Figure 4, Figure 5, Figure 6, Figure 7).

Movement at plate boundaries is seen and felt along faults. The materials along the boundaries of these plates are continuously being squeezed and sheared, causing them to bend and break (Wood and Kienle 1990). Stresses build along edges of the plates until part of the crust suddenly gives way in a violent movement causing a sudden release of stored energy, radiating outward from the fault in what is known as an earthquake. Most earthquakes are so small that special instruments are needed to detect them, but a few release huge amounts of energy, causing widespread destruction (Wood and Kienle 1990). During most earthquakes, fault motion stays below the Earth's surface, but in large earthquakes, fault motion may break through to the surface and be felt for dozens or hundreds of miles away (USGS 2010).

The pattern of stress in the crust changes over geologic time, faults are formed, slip for a time, and then retire (USGS 2010). Geologists focus their studies on Quaternary-active (the last 1.6 million years) faults, which have ruptured in Quaternary time. Faults that have not broken in the last 1.6 million years are probably abandoned, or at least they cause an earthquake so infrequently as to be less of a concern today. On the other hand, faults that have ruptured in Holocene time (the last 11,500 years - Figure 2) are considered the most active faults.

Figure 4. Cascadia subduction zone and shifting plates along the Pacific Ocean shoreline to the North American continent (reproduced from USGS 2010).

Cascadia earthquake sources

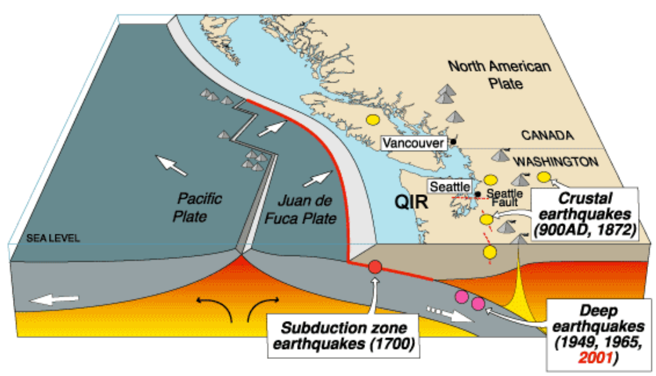

Source	Affected area	Max. Size	Recurrence
Subduction Zone	W.WA, OR, CA	M 9	500-600 yr
Deep Juan de Fuca plate	W.WA, OR,	M 7+	30-50 yr
Crustal faults	WA, OR, CA	M 7+	Hundreds of yr?

2.2.1. Cascadia Subduction Zone

The Cascadia Subduction Zone (CSZ) is the result of a convergent plate boundary between Juan de Fuca oceanic crust and North American continental crust. The CSZ starts with the Juan de Fuca Ridge where the Pacific Plate, Juan de Fuca Plate, Explorer Plate, and Gorda Plate are formed (Figure 4 & Figure 7). The oceanic crust of the Juan de Fuca plate is subducted beneath the continent at a rate of about 30-40 mm/yr (Wood and Kienle 1990, Hellwig 2010, Kirby, Wang and Dunlop 2002). The Juan de Fuca Plate (Figure 7), has small platelets (plate fragments that have separated from the larger plate) at its northern (Explorer Plate) and southern (Gorda Plate) terminations. The Explorer Plate separated from the Juan de Fuca plate approximately 4 million years ago and is apparently no longer being subducted. The Gorda Plate split away between 18 and 5 million years ago (Hyndman, Davis and Wright 1979) and the subduction process continues. The width of the CSZ varies along its length, depending on the temperature of the subducted oceanic plate, which heats up as it is pushed deeper beneath the continent. As it becomes hotter and more molten, it eventually loses the ability to store mechanical stress and, as it happens, earthquakes are generated (NGDC 2010).

Tectonic processes active in the CSZ region include subduction, accretion, deep earthquakes, and active volcanism (Kirby, Wang and Dunlop 2002) that has included such notable eruptions as Mount Mazama (Crater Lake) several thousand years ago and Mount St. Helens in 1980 (Geller 2008).

The entire extent of the region that today is called the Olympic Peninsula, is a conglomerate of sediment cover materials that were scrapped off the eastern moving oceanic Juan de Fuca Plate under the North American continental Plate beginning at the CSZ deformation front (Figure 5). Those abraded materials contain sand, silt, chunks of basalt, organic matter, glacial till, glacial erratics (boulders), and even materials such as volcanic ash released from on-shore volcanoes (like Mount St. Helens and Mount Mazama), that were carried to the ocean by wind and rain erosion, and glacial deposition carried by rivers and glaciers to the ocean. Seaside cliff materials are also deposited into the ocean as a normal course of events. The mélange of materials includes water particles; both salt water and fresh water. This accumulation of materials has been uplifted, tilted, and deformed into mountain ranges. The sediment cover over the Juan de Fuca Plate has a thickness of up to 2,500 m (Hellwig 2010).

Figure 5. The Cascadia Accretionary Wedge and the Juan de Fuca Subduction Zone (Hellwig 2010).

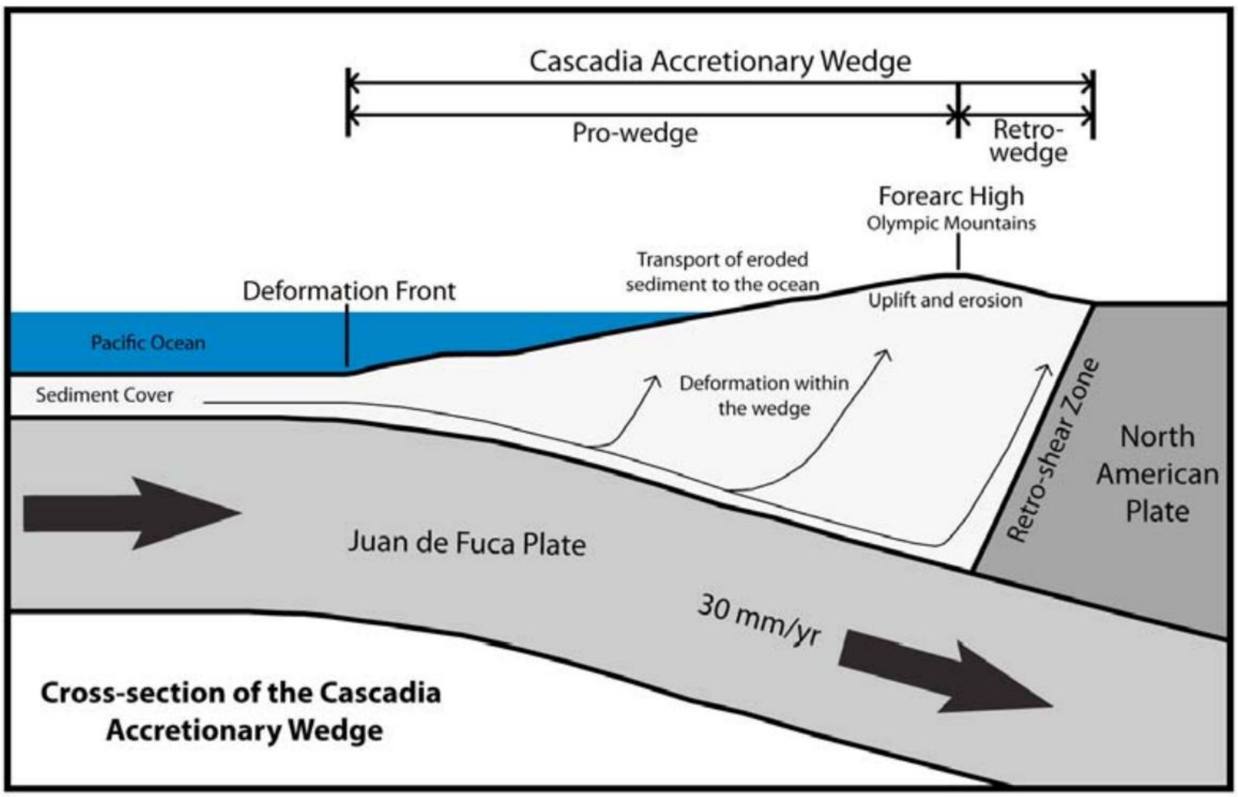

The materials scrapped off the oceanic plate are pressed together, deformed, squeezed, and held under pressure. The materials of the mélange are capped, much like a stew in a pressure cooker. The heat for this pressure cooker comes from the abrasive motion of the tectonic plates rubbing and pushing against each other (Holdahl, Faucher and Dragert 1989), from the pressurized forces of the overburden capping these materials, and from the decomposing organic matter of the detritus held in this stew. These forces result in compression as the water and other materials expand making the pressure cooker’s lid ultimately blow off.

The release of pressure can cause mud volcanoes to erupt below sea, or on land. The Garfield Gas Mound near Taholah is one example of this type of pressure release point for the forces below (Rau 1973). Although the gas emitted from this mud volcano smells bad (stink muds), it is not a volcano in the same way that Mount St. Helens or Mt. Rainier are volcanoes; those are andesite stratovolcanoes.

The oldest subsurface materials of the Olympic Mountains are adjacent to Hood Canal (Williams 2002). The deformation wedge layers become progressively younger the further you move west. At the peak of Mount Olympus a climber can locate an ancient ocean floor fossil group of extinct marine arthropods that form the class Trilobita. Trilobites form one of the earliest known groups of arthropods and lived about 521 million years ago and became extinct about 250 million years ago (Levi-Setti 1995). Their presence along the Olympic Mountains is evidence to the fact that the peaks of the Olympics have been uplifted to their current heights from the ocean floor (Eaton and Fredricksen 2007).

2.2.2. Earthquakes

Periodic giant megathrust earthquakes in this region happen as a result of these tectonic processes. In the period between the mega-earthquakes, the Juan de Fuca plate continues to slide beneath the North American plate with the consequence that the rocks along the edges of the plates are compressed or squeezed and uplifted. Knowing where and how fast the rocks are being deformed enables us to estimate the approximate width and length of the fault that may slip in the next megathrust earthquake. Another reason for determining how crustal deformation varies from place to place in the subduction zone is the need to know how and where the stress is changing so we can predict large crustal earthquake events.

Elastic deformation builds up between great earthquakes when the joining of two plates becomes locked into what is called a “thrust fault”. Along the QIR shorelines, the western side of the deformation wedge (Figure 5) is dragged down and a flexural bulge forms (Figure 6). When the lock between the plates is released, it causes the seaward edge to collapse at the flexural bulge, causing a great earthquake which can also generate a tsunami. The collapse of the bulge can cause subsidence resulting in the formation of buried coastal marshes (Eaton and Fredricksen 2007, Geller 2008). Historically, along the QIR marine coastline these bulge uplifts and subsidence ruptures have happened (see Section 2.2.4 & Figure 8). They are happening now with both uplift and subsidence events apparent along the marine shorelines of the entire coastline (see Section 3.2.1).

Figure 6. Land deformation caused by Subduction Zone Processes (Hyndman, Rogers, et al. 2008).

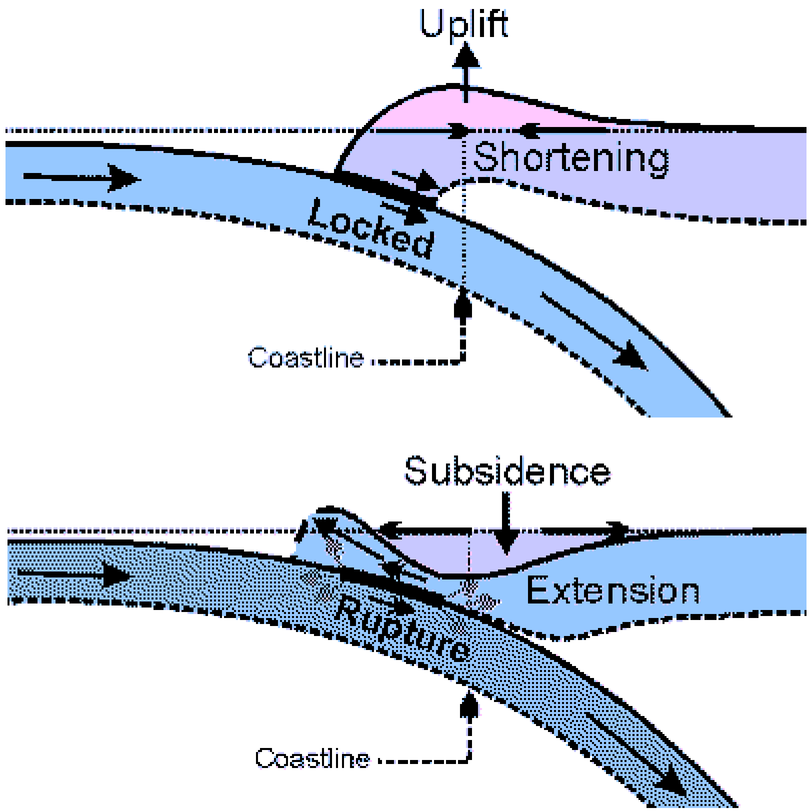

The motion of the subducting Juan de Fuca plate is influenced by changes in frictional resistances. Since it does not move as one solid sheet of basalt, the movement is slowed on one face, while it moves freer on another face, causing fractures along the plate. These fractures are called fault lines. Some of these fractures are horizontal fractures, while others are vertical, but most faults are a combination of the two.

"Megathrust" events have historically occurred offshore within the subduction fault zone and can be catastrophic (magnitude 9 on the Richter Scale). The last such megathrust event along this coastline occurred approximately 300 years ago and created a tsunami felt locally and a tsunami wave that travelled across the Pacific Ocean to Japan (CREW 2005). While relatively infrequent, the megathrust earthquakes have a fairly well documented return interval of 400 to 600 years (NGDC 2010). Researchers believe that strain within the locked zone of the subduction fault is currently building (Figure 7), and as it does, the likelihood of a major subduction earthquake event increases. More common earthquakes occur within the subducting oceanic crust, or within overlying continental rocks, and the 2001 Nisqually earthquake with an epicenter near Olympia, provides a recent example.

More than 1,000 earthquakes occur in Washington State annually. Washington has a record of at least 20 damaging earthquakes during the past 125 years. Large earthquakes in 1946, 1949, and 1965 killed 15 people and caused more than $200 million (1984 dollars) in property damage (WaDNR 2010). Most of these earthquakes were in western Washington, but several, including the largest measured historic earthquake in Washington (1872), occurred east of the Cascade crest (USGS 2010). All the Quaternary-active faults in the Juan De Fuca plate region are part of the CSZ system and are considered active (WaDNR 2010).

Figure 7. Tectonic Profile (NRC 2008).

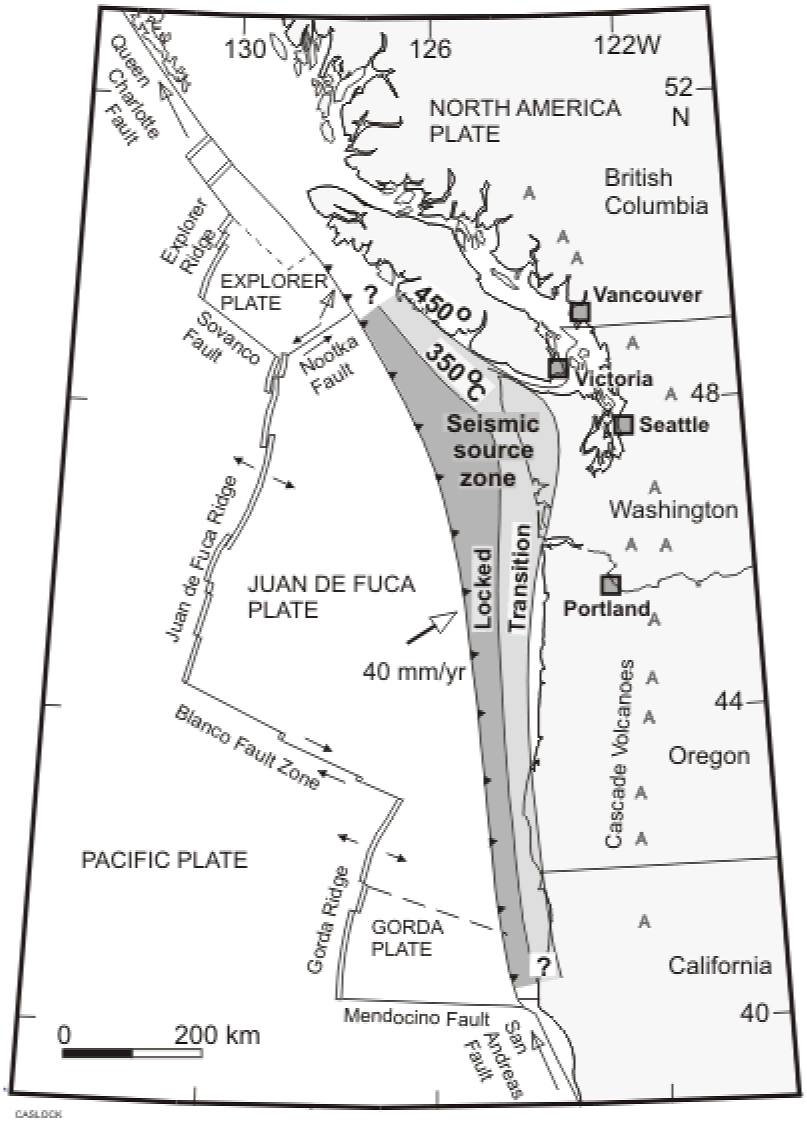

2.2.3. Faults

The WaDNR, Division of Geology and Earth Resources, created geospatial data containing Quaternary fault lines for the state of Washington and offshore areas. This digital dataset shows the location of faults with known or suspected Quaternary (<1,600,000 yrs) activity in the state of Washington. Data was gathered from numerous sources, including the Washington state portion of the U.S Geological Survey's "Quaternary fault and fold database of the United States" (USGS 2009). Faults were attributed with information such as age, visibility, method of detection, and in most cases, the corresponding ID number for the fault in the USGS database, for easy correlation between the two data sources (WaDNR 2010). These data sources have been used to document the location and characteristics of fault lines in and near the QIR.

There are 261 Quaternary fault lines within 100 miles of the exterior boundaries of the QIR. Selected from these faults, are approximately 66 faults that are located within the QIR or to the west of the QIR all the way to the CSZ (Table 1). Some of these fault lines are very young, formed within the last 15,000 years, and some of those faults are located very near the QIR (e.g., unnamed faults near Duck Creek). A series of these faults are located between Taholah and Qui-nai-elt, including Point Grenville.

Table 1. Faults within the QIR and westerly of the QIR.

Fault Name	Age	Distance From QIR (miles)
Unnamed fault near Wreck Creek	<130,000	0
Unnamed fault zone near Raft River	<130,000	0
Unnamed fault zone near Raft River	<750,000	0
Unnamed fault zone near Raft River	<750,000	0
Unnamed fault near Wreck Creek (Class B)	Unknown	0
Unnamed faults near Duck Creek	<130,000	1
Unnamed faults near Duck Creek	<130,000	1
Unnamed fault zone near Raft River (Class B)	Unknown	1
Unnamed faults near Duck Creek	<15,000	2
Unnamed fault zone near Aloha (Class B)	Unknown	2
Unnamed fault zone near Aloha	<15,000	3
Unnamed fault zone near Aloha (Class B)	Unknown	3
Unnamed fault zone near Aloha	<1,600,000	4
Unnamed faults offshore of Queets River	<1,600,000	5
Unnamed faults offshore of Queets River (Class B)	Unknown	6
Unnamed fault zone near Langley Hill (Class B)	Unknown	7
Unnamed fault zone near Aloha	<130,000	8
Langley Hill fault	<1,600,000	9
Unnamed fault zone near Langley Hill	<130,000	9
Unnamed fault zone near Langley Hill	<15,000	11
Saddle Hill faults	<1,600,000	12
Unnamed faults offshore of Queets River	<15,000	12
Saddle Hill faults	<1,600,000	13
Saddle Hill fault zone	<130,000	13
Unnamed fault zone near Langley Hill	<130,000	14
Saddle Hill fault zone	<750,000	14
Saddle Hill fault zone (Class B)	Unknown	15
Grays Harbor fault zone	<1,600,000	16
Unnamed fault zone near Langley Hill	<15,000	16
Saddle Hill fault zone	<130,000	18
Grays Harbor fault zone	<15,000	18
Grays Harbor fault zone	<130,000	19
Saddle Hill fault zone	<15,000	19
Grays Harbor fault zone	<1,600,000	25
Unnamed offshore faults near Grays Canyon	<130,000	25
Unnamed faults near mouth of Willapa Bay	<130,000	26
Unnamed faults near mouth of Willapa Bay	<1,600,000	31
Unnamed fault zone offshore Cape Shoalwater	<1,600,000	32
Unnamed fault zone offshore Cape Shoalwater (Class B)	Unknown	33
Unnamed offshore faults near Grays Canyon	<15,000	34
Unnamed offshore faults near Grays Canyon	<130,000	35
Willapa Bay fault zone	<130,000	35

Table 1. Faults within the QIR and westerly of the QIR.

Fault Name	Age	Distance From QIR (miles)
Unnamed faults near mouth of Willapa Bay (Class B)	Unknown	35
Willapa Bay fault zone	<130,000	36
Willapa Bay fault zone	<130,000	36
Willapa Bay fault zone	<130,000	38
North Ninitat fault zone	<15,000	40
Unnamed offshore faults near Grays Canyon	<130,000	41
Willapa Bay fault zone	<130,000	43
Unnamed offshore faults near Grays Canyon	<15,000	46
Willapa Bay fault zone	<750,000	51
Unnamed offshore faults near Grays Canyon	<130,000	53
South Ninitat fault zone	<750,000	53
Willapa Bay fault zone	<750,000	54
Nehalem Bank fault	<15,000	63
North Ninitat fault zone	<15,000	63
North Ninitat fault zone	<15,000	67
South Ninitat fault zone	<750,000	67
Fault J	<15,000	68
Unnamed offshore faults	<15,000	74
Willapa Canyon fault	<1,600,000	81
Cascadia fold and thrust belt	**<15,000**	**81**
Cascadia Subduction zone	**<15,000**	**81**
South Ninitat fault zone	<750,000	81
Nehalem Bank fault	<15,000	83

2.2.4. Quinault Marine Shoreline Tsunami Impacts

Quinault marine shorelines have witnessed tsunami events. The principal cause of a tsunami is the displacement of a substantial amount of water. This displacement of water is usually attributed to either earthquakes, landslides, volcanic eruptions, glacier calvings or more rarely by meteorites and nuclear tests (Margaritondo 2005). The waves are sustained by gravity. Tides do not play any part in the generation of tsunamis. The historic tsunamis along the Quinault marine shoreline may or may not have been triggered by local earthquakes.

When an earthquake happens within the CSZ, the release of stresses within the Juan de Fuca plate, and the accretionary wedge forming the Olympic Mountains, causes movement of the ocean floor and a tsunami wave can be generated. Tsunami can be generated when the sea floor abruptly deforms and vertically displaces the overlying water. Tectonic earthquakes are a particular kind of earthquake that are associated with the Earth's crustal deformation; when these earthquakes occur beneath the sea, the water above the deformed area is displaced from its equilibrium position (UW 2012). More specifically, a tsunami can be generated when thrust faults associated with convergent or destructive plate boundaries move abruptly, resulting in water displacement.

Movement on normal faults will also cause displacement of the seabed, but the size of the largest of such events is normally too small to give rise to a significant tsunami. These tsunami waves can move quickly and inundate the shorelines with the displaced ocean water. The impact area can be local, or involve the Pacific Ocean shoreline for about 200 miles (Margaritondo 2005).

A Federal Indian Agent report, from Taholah, written on May 7, 1887, reads, “Something like a tidal wave struck the Quinault Agency at midnight. Some of the Indian houses were waist deep in water, the inmates yelling in terror as they were submerged during sleep on their low sleeping places. The water receded as rapidly as it came, carrying everything portable in its exit”. On December 24, 1920, media reports state, “a small tidal wave sweeps beaches, washes 12 Sunset Beach cottages from their foundations” (Workman 2010). These events most likely described local earthquakes along the Juan de Fuca plate and within the CSZ interface that impacted the Quinault shorelines specifically.

Workman (2010) includes reports that were conveyed from local media, that “a five foot high tidal wave races up the Quinault River” on April 1, 1946. This tsunami event was recorded as a result of an earthquake at Unimak Island in Alaska. This event was a basin-wide impact in response to a megathrust event originating in Alaska.

The March 28, 1964, tsunami was felt strongly along the QIR shorelines where bridges were washed out, roads were made impassable from debris and seawater. North Beach was hit by a tsunami wave destroying Joe Creek and Copalis Beach bridges. The height of the run-up along the shore was highly variable with Wreck Creek and Moclips witnessing the highest waves locally at 11 feet and 15 feet respectively. Slightly to the north of these shorelines, at Taholah, the run-up height was only 2.4 feet (Schlosser 2010).

The Washington coastline has witnessed approximately 22 tsunami events from 1900 to present time. Since the development of tsunami travel time charts for the Pacific and the Pacific Tsunami Warning Center’s development after 1964, the ability to track tsunami events in real time has increased the accuracy and reporting of these data. Tsunami events reported prior to 1964 relied mostly on printed records and reports concerning tsunami events and on scientific investigations to estimate where tsunami events initiated and where data show that tsunami run-ups were witnessed (often times using tsunami deposits as an indicator).

Some of the most convincing and best-preserved evidence of the tsunami(s) are sand layers that cover the peaty soils of coastal lowlands. Large tsunamis can deposit seafloor derived sediment layers on the inundated coasts bordering the fault zone. The last confirmed CSZ-related earthquake occurred in 1700 and resulted in sudden land subsidence of 1 meter (3.3 ft) or more (Leonard, Hyndman and Mazzotti 2004, Jacoby, Bunker and Benson 1997). One of the surges along the Oregon coastline picked up sand from the beach or dunes as it came ashore and deposited the sand as it moved up the river valley (Figure 8). At the site of the photo, the sand bed covers the remains of two fire pits, perhaps used not long before the tsunami struck. The layers are well preserved partly because much of this part of the Oregon coast permanently subsided about 0.5-1.0 m (2-3 ft.) during the earthquake (see Figure 6 for an illustration of this process). The rise in relative sea level produced by the land’s subsidence allowed tidal sediments to quickly bury the sand layers, protecting them from later erosion (USGS 2009).

Figure 8. This photo (USGS 2009) shows a sand layer in an exposure near the mouth of the Salmon River along the central Oregon coast about 8 km (5 mi) north of Lincoln City with tsunami delivered sand overtopping fire pits.

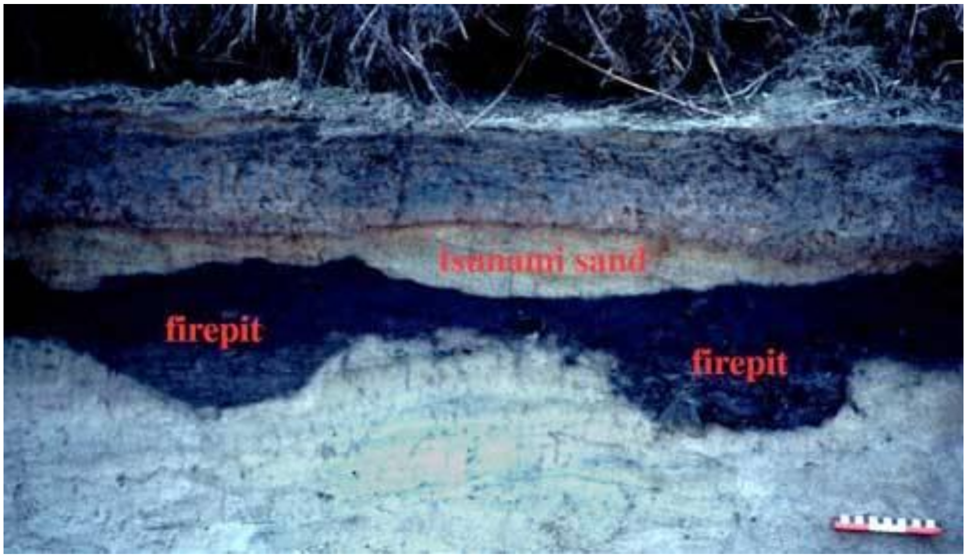

The 1700 tsunami has been linked with flooding that drowned entire forests along the Washington, Oregon, and British Columbia coastlines, and deposited sand on marshes and in lakes along the southern part of the CSZ coast. It is believed that a sand sheet at Discovery Bay in the Straights of Juan de Fuca was also placed by this 1700 tsunami (Atwater, et al. 2005, WSMD 2009).

Based on geologic evidence and scientific interpretation, the CSZ has experienced major ruptures and created tsunamis at least 7 times in the past 3,500 years and has a considerable range in recurrence intervals, from as little as 140 years between events to more than 1,000 years. Researchers predict a 10 to 14% chance that another tsunami generating earthquake could occur in the next 50 years within the CSZ (Wood and Soulard 2008, WSMD 2009).

2.2.5. Bathymetry Profiles

A bathymetry profile of the seafloor from slightly west of the CSZ to the shoreline at Taholah (Figure 9) shows elevation changes (bathometry) along this path (Figure 11). This transect line reveals the undersea rise, peaks, canyons, and climb to the shoreline. This profile shows a 2,500 meter (8,200 foot) elevation ascent from the Juan de Fuca plate floor to the current coastline spread over a distance of 112 miles.

This particular profile (Figure 11) shows several interesting events. First, in the distance between 35,000 and 80,000 meters from the western edge of the profile, we can see several peaks of accretionary prisms and subduction-complex basements. These have been formed along the Juan de Fuca Plate between the Juan de Fuca Ridge and the CSZ. The oceanic plate is saturated with water, and volatile materials such as water drastically lower the melting point of the mantle (Grove, et al. 2006). As the oceanic plate keeps subducting, it gets subjected to greater and greater pressures with increasing depth. This pressure squeezes water out of the plate and introduces it to the mantle. At this point the mantle melts and forms magma at depth under the overriding plate. Sometimes, the compaction, heat, and friction can cause premature melting of the Juan de Fuca Plate triggering materials to expand upward along fault line crevices in the process of relieving the mounting pressure.

The amalgam of materials (sedimentary deposits) settling on top of the Juan de Fuca plate force severance of the basaltic 'stacks' where the crags become part of the geologic mélange forming the Olympic Mountains. These fragments are seen along the Quinault coastline in the form of basaltic islands and erosion resistant points mixed with glacial erratics (boulders) in such locations as Hogsback and Point Grenville. Although these features are 1) erosion resistant basalt formed at depth and 2) glacial erratic materials, they are not physically attached to the Juan de Fuca Plate as it is subducted under the mantle.

Another conspicuous feature of this profile (Figure 9) is seen in the distance between 100,000 meters and 135,000 meters from the initial point: Quinault Canyon. This offshore canyon is displayed from the 'mouth' of the canyon to its undersea 'ridgeline'. The Quinault Canyon is a complex of glacially carved features containing a mixture of soft sediments, with cobble and boulder patches, and scattered large glacial erratics (boulders) deposited during ice retreat. High-relief, submerged topographic features serve as fish aggregation areas.

Low-resolution surveys of this seafloor have revealed a generally wide and featureless continental shelf dominated by soft substrates (sand and mud bottoms, to pebble and cobble) with scattered areas of rock outcrop and basaltic spires (USGS 2010, Verdonck 2006).

2.2.6. Topographic Profiles

The topographic profiles (Figure 12) of the Quinault mainland are shown along a transect line (Figure 10) from Taholah up the general path of the Quinault River, through Amanda Park, generally along the Upper Quinault river until its zenith is reached at Mount Anderson. This profile shows a relatively horizontal ascent from Taholah to the glacial moraine's terminus near Amanda Park. At this point the elevation starts to climb rapidly with the reach achieving its final point at Mount Anderson.

All of the substrate materials of this profile are composed of sand, silt, chunks of basalt, organic matter, glacial till, glacial erratics and other materials that begin their accumulation near the CSZ.

Figure 9. Profile line overview of seafloor bathymetry shown in Figure 11.

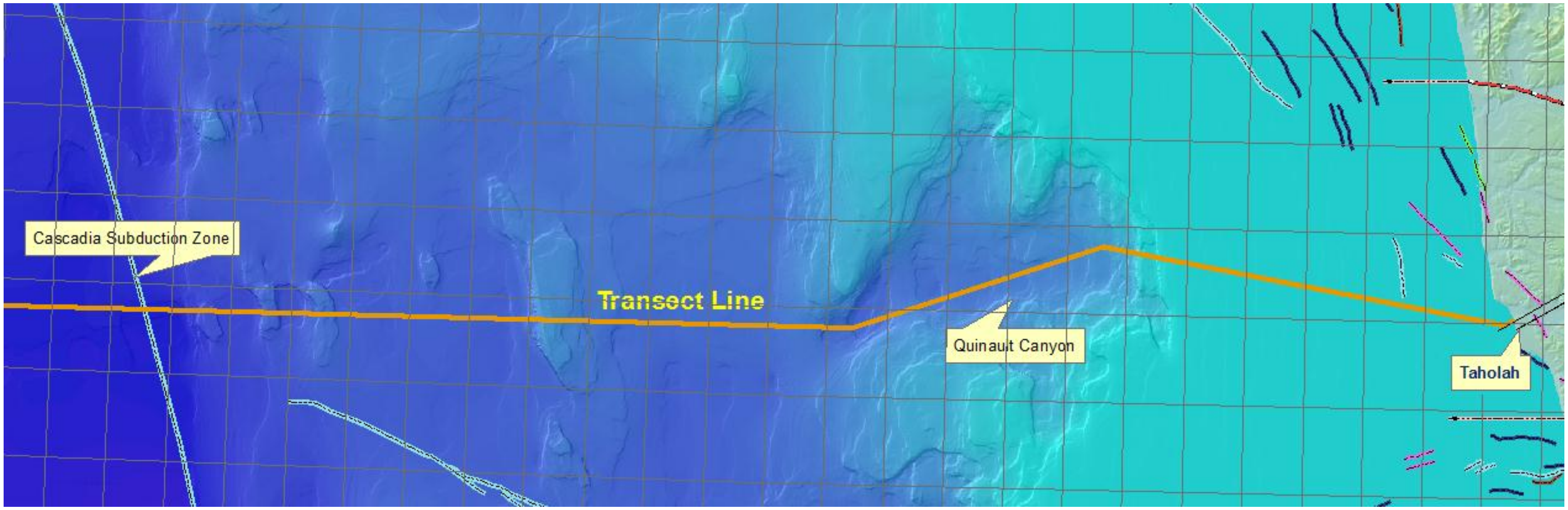

Figure 10. Profile line overview of topography shown in Figure 12.

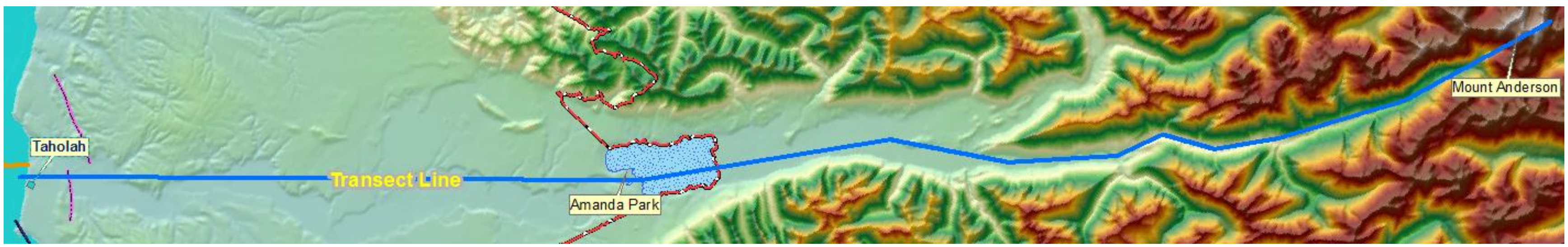

Figure 11. Seafloor bathymetry profile line from Juan de Fuca plate to Taholah as displayed on Profile in Figure 9.

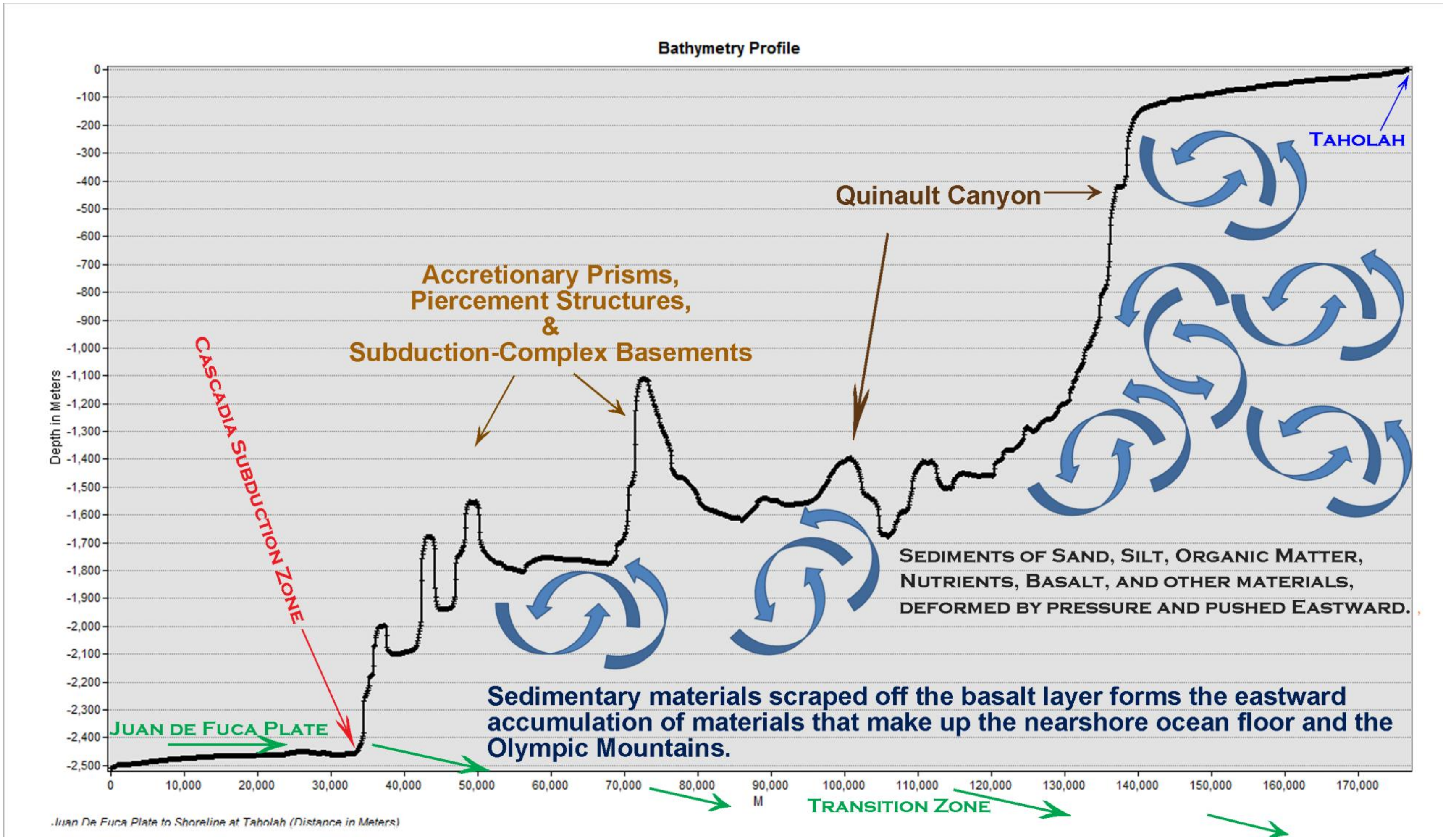

Figure 12. Topographic profile line from Taholah to Mount Anderson as displayed on profile in Figure 10.

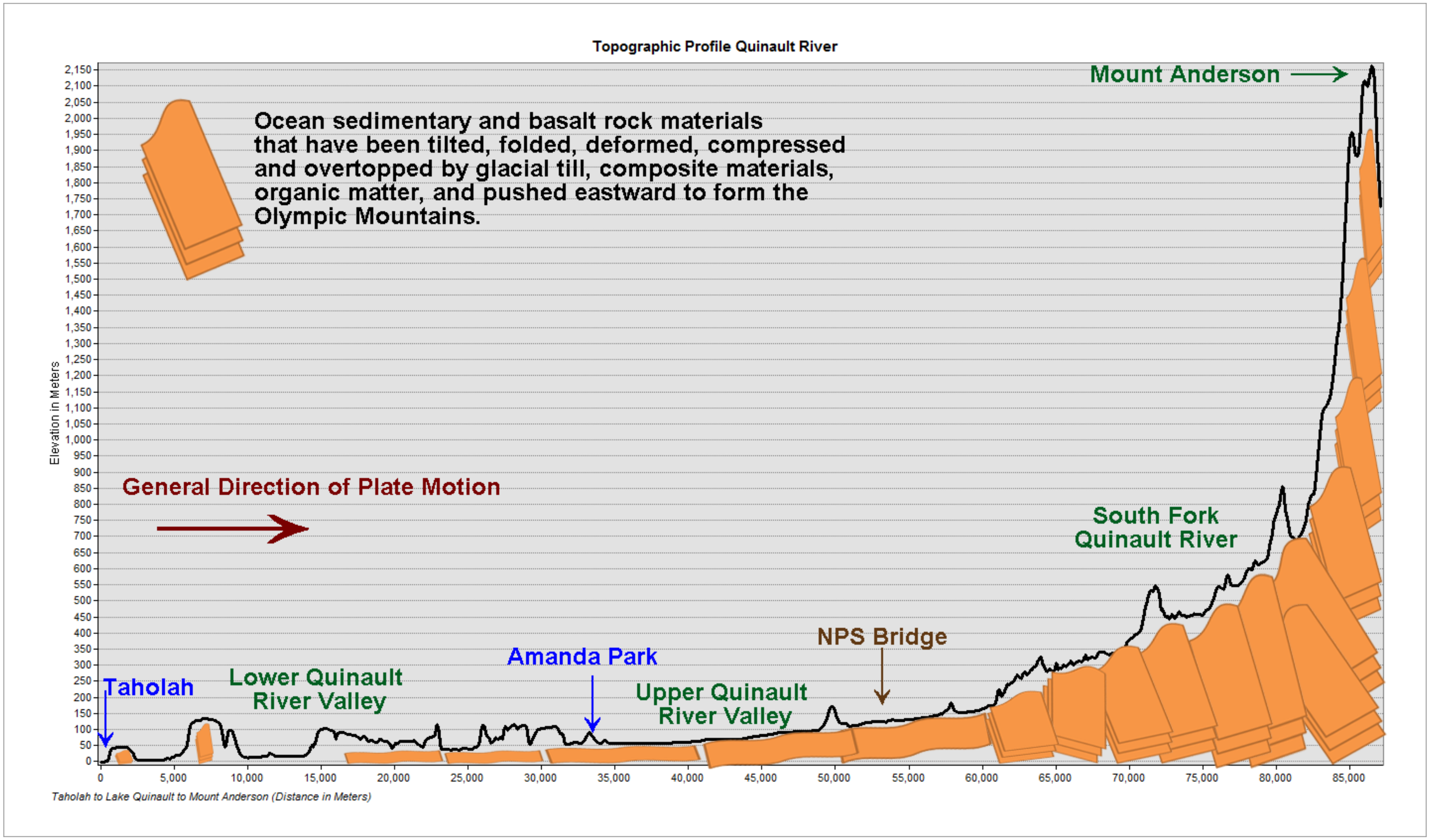

2.3. Littoral Cells, Beaches, and Sand

The littoral systems found within the QIR marine shorelines define the topographically influenced delivery of nutrients, sand, particulate matter, and other materials past the mouth of each river as they enter the ocean. After entrance to the ocean, the delivery of river borne materials is influenced by near-shore ocean bathymetry with the seasonally influenced ocean current patterns. The coastal zone as a whole, is a dynamic environment within the land-water boundary and contiguous land forms are continuously modified and realigned by the forces of the sea. It is important to identify, recognize, and understand the shoreline boundaries and mechanisms of drift sectors that serve an important role in beach formation and erosion.

2.3.1. Local Littoral Cells

The QIR coastline is divided into a set of distinct, self-contained littoral cells or beach compartments (Moclips River, Quinault River, Queets River, etc.). These compartments are geographically limited, based on the shape of the offshore bathymetry, relative size of the contributing watersheds and consist of a series of beach sediment (commonly referred to as just 'sand') sources (such as rivers, streams and eroding coastal bluffs). Sand sinks (such as coastal dunes and submarine canyons) where beach sediments are lost from the shoreline, and longshore transport or littoral drift moves beach sediments along the shoreline. Sediment within each cell includes the sand on the exposed or dry beach as well as the finer-grained sediment that remains offshore (Patsch and Griggs 2006).

Beach sand moves on and offshore seasonally in response to changing wave energy, and also moves alongshore, driven by waves that usually approach the beach at some angle. Most QIR marine coastline beach sand is transported from south to north as a result of the dominant waves approaching the shoreline from the southwest.

2.3.2. Columbia River Littoral Cell

There is one littoral cell that is a dominant feature along the southern QIR shorelines and it comes from off-Reservation; the Columbia River Littoral Cell (CRLC). The large Columbia River watershed basin carries sediments from about 260,600 square miles in Washington, Oregon, Idaho, Nevada, Utah, Wyoming, Montana, Alberta, and British Columbia. The Columbia River watershed is the 3rd largest watershed in the United States by water discharge volume (USGS 2012).

Historically the ocean shorelines of southwest Washington and northwest Oregon expanded at rates exceeding several meters per year. These high accretion rates have been credited to large supplies of sand from the Columbia River. This widespread accretion resulted in new coastal lands, on which public and private infrastructure and facilities have been built. This zone extends from the Columbia River northward to Point Grenville with effects seen as far north as Taholah and the mouth of the Quinault River.

The extensive construction of hydroelectric dams along the Columbia River (eleven major and over 200 smaller dams in the mid-1900s) has interrupted the sediment delivery from the watersheds of that region. Since the 1950s, the amount of sediment from the CRLC delivered to the Pacific Ocean shorelines in Washington and Oregon has dropped considerably (Gelfenbaum, et al. 1999). The causes of this reversal from accretion to erosion include dam construction along the Columbia River system, and human activities such as off-shore dredging for seaport water vessel traffic and jetty construction (Phipps 1990).

The CRLC has been segmented into four arc-shaped sub-cells; North Beach extends formally to Point Grenville, but has extended influences, when combined with local littoral zone sediments, as far as the mouth of the Quinault River. The finest sand particles within the CRLC are found the furthest from the mouth of the Columbia River. Further modifications to the shores of this North Beach CRLC are seen by wave terrace structures resulting from several cycles of differentiated CRLC variations.

Deep offshore basins extend close to QIR shores and serve as effective barriers to littoral drift thus terminating most littoral cells. The Quinault Canyon (Figure 9) is the largest permanent sink for sand near the QIR. Sand accumulates at the head of this canyon and, through underwater sand flows and turbidity currents, is funneled away from the shoreline (Patsch and Griggs 2006), until repatriated to the shorelines by seasonal changes in upwelling currents.

2.3.3. Overlapping Littoral Cells

The CRLC is the largest littoral cell contributing sediments to the QIR marine shorelines. The local littoral cells (collectively henceforth called the Quinault Indian Reservation Littoral Cells - QIRLC) provide unique sediment contributions to the marine shorelines. Littoral cell sediments include particles as small as clay and silt, fine-to-coarse sands, pebbles to gravel, cobbles, and even boulders. Sediment is transported based on the strength of the flow that carries it, and the particle's size, volume, density, and shape.

The sediments delivered by the CRLC are mostly derived from terrain overtopping and cutting through the continental batholith. The batholith is formed from igneous intrusive (also called plutonic) rock that forms from cooled magma deep in the Earth's crust. Batholiths are almost always made mostly of felsic or intermediate rock-types, such as granite, quartz monzonite, or diorite. The sediment of the Columbia River with eroded materials of the continent is carried to the ocean shorelines.

The rivers of the QIR deliver the sediment first eroded, then transported, from the lands of the Olympic Peninsula accretionary wedge. The sediments from these rivers do not contain granite particles to make sands like the CRLC does. The QIRLC contains a high concentration of organic material (slightly decomposed plant materials) within the matrix of environments they erode (NRCS Soil Survey Staff 1999). The QIRLC river systems drain lands from currently glaciated environments, through recently glaciated ecosystems, including lush forestlands. These contributing watersheds contain a mix of silts, clays, and sands in combination with silt loam, peat, and slightly decomposed plant materials.

The delivery of these sediments provide the organic nutrition for macroinvertebrates. The unique combination of the CRLC and QIRLC sediments creates the nutrition for clams with the substrate to support their preferred habitat. Due to this unique combination, the macroinvertebrates (such as razor clams) find the most successful habitat in the world in some locations of the QIR shoreline. North of Taholah the CRLC sediments are not found. South of Copalis Beach the QIRLC sediments do not extend.

2.4. Macroinvertebrate Resources of the Outer Coast

Detailed information on historic and current conditions in the Juan de Fuca Plate's seafloor marine macroinvertebrate habitat is limited due to technological challenges and associated costs. Thus, to a large extent the current condition of seafloor habitats must be inferred. The most widespread negative impact to seafloor habitats is likely to have resulted from the bottom trawl fishery using gear known to reduce seafloor complexity, alter the physical structure of seafloor habitats, and damage biogenic habitat, or habitat formed by living organisms, such as corals and sponges (Auster and Langton 1999, Norse 1994, Thrush and Dayton 2002, Olympic Coast National Marine Sanctuary 2011).

The major relevant features of the northern QIR marine shorelines include high tidal range, strong wave action, and an unusual shoreline which provides limited opportunity for the development of sandy substrates suitable for the development of shellfish beds. Pocket beaches that do exist tend to be small in size and are dominated by sand and gravel and influenced by major river drainages, such as the Queets River and Quinault River. Due to the variation in surface structure of the marine coastline, the abundance and diversity of invertebrate resources is relatively low, particularly for large, edible molluscan resources. North of Cape Elizabeth, shellfish available for human consumption are those that have adapted to high-energy, rocky habitats (Schalk 1988). South of Point Grenville, habitat for razor clams exceeds productivity to eclipse most other locations in the world for their proliferation.

Because of the frequency of wintertime storms generated in the southwestern Pacific Basin that are delivered to the Quinault shorelines (Mass 2008), it is the northward current that carries the most concentrated sediment load to the shorelines. During the summer months, a general upwelling of water from lower depths in the Quinault Canyon (Figure 9) is seen. The upwelling water is cold, high in salinity, low in oxygen, and rich in nutrients (many which have been sequestered in the littoral cell sink of the Quinault Canyon). The biogenic bloom triggered when the summer currents reverse, creates vegetative life beneficial to razor clams and many other marine creatures, including crabs.

Steelhead trout, blueback, Chinook, coho, and chum salmon seek the nutrients, clear waters, and other resources combined in this area, making it remarkable salmon habitat. Humpback and Orca whales, porpoises and dolphins pass through the area, often quite close to shore, on their annual migrations.

The steepness of the offshore gradient, particularly in the portions north of Cape Elizabeth, results in a reduction of diverse shellfish habitat. The steepness of the offshore gradient and the high wave energy causes invertebrate habitat segregration such that few areas show overlapping eco-zones (Rigg and Miller 1949). The seasonal upwelling systems within the off-shore environment have reduced the abundance and diversity of invertebrate resources along the Quinault Marine coastlines.

The Moclips River to Point Grenville portion of the North Beach CRLC is notable for their abundance of shellfish. It is expected that a reduction in sand loading along the extended coastline (CRLC) could cause reductions in mollusk populations that rely on those habitat resources. Mollusk habitat within the intertidal and subtidal communities of the QIR marine shorelines is seen in five major shellfish associations, three of which dominate in rocky, high-energy zones (north of Cape Elizabeth), and two thrive in the sandy zones common south of Cape Elizabeth (Wessen 1977, Schalk 1988).

2.4.1. Sea Mussel-Gooseneck Barnacle Association

The Sea Mussel-Gooseneck Barnacle (*Mytilus californianus-Pollicipes polymerus*) association dominates in high energy, rocky intertidal zones. High-energy resistant species such as limpets (*Acmaea spp.*), barnacles (*Mitella spp., Balanus spp.*), and giant chitons (*Katharina tunicata*) are found with this group and find a niche in the high energy shorelines. Seas-mussel "mats" of up to 25 cm thickness develop as individuals utilize threads to attach themselves to bare rock surfaces (Dayton 1971) (such as to the strata found between the Hogsback area and Cape Elizabeth). As a food source, the mussels, limpets, and chitons have been considered a highly concentrated food source that also requires little harvest 'expense' to convert them to foodstuffs. Barnacles attach tightly to rocks and have a low nutrient yield in comparison to the other harvestable seafood members of this association. Despite this, the habitat's overall biomass concentration of appetizing seafood is considerable (Schalk and Yesner 1988). Barnacles have historically been harvested along the Quinault coastlines and continue to be harvested now.

One resident species within this association is the ochre starfish (*Pisaster ochraceus*) (Figure 13). Mills Soule, and Doak (1993) made reference to this species when describing the Keystone-species concept in intertidal zones. This colorful starfish can be abundant and can thrive in the high-energy shoreline environments, especially where rocky substrates are found. The ochre starfish is a predator of the common mussel and reduces its abundance. The increase, or decrease, of this species' abundance will lead to changes in the intertidal species diversity.

Studies of the ochre starfish concluded that it will not be affected by ocean acidification in the same way as most calcerous marine animals (Gooding 2009). Increased acidity created from dissolving calcium carbonate causes decreased growth in mollusks. This same conclusion was not observed in tests to the ochre starfish. Findings concluded that it can compensate for the lack of carbonate by increasing its fleshy tissue and therefore not be affected by climate change and ocean acidification in the same way as cohort species in this association.

Figure 13. Ochre sea stars, also known as ochre starfish (Pisaster ochraceus) found within the Quinault marine shoreline habitats (Workman 2012).

2.4.2. Bent-nose Clam-Mossy Chiton Association

The Bent-nose Clam-Mossy Chiton (*Macoma nasuta-Mopalla muscosa*) association is found where moderate wave-energy zones are correlated with the commonly found wave-cut rock platforms of the Quinault Marine Shorelines from Cape Elizabeth to Whale Creek. Where these habitats correspond with intertidal pools, the members of this community usually appear as individuals rather than as aggregates in large groups. Often they are scattered with large breaks between community member collections. As individuals, the community members are generally relatively small, low-yield organisms. Some non-shellfish invertebrates are found within this zone and include the Rock Crab (*Cancer productus*) and the North Pacific Octopus (*Octopus dofeini*)) (Schalk and Yesner 1988). Because of the higher energy cost of harvesting these seafood sources, their collection has faced a lower intensity. Harvest has been taken as an opportunistic or targeted collection of rock crabs, octopus, and occasional clams and chitons.

2.4.3. Little-neck clam - Butter Clam - Horse Clam Association

Suitable habitat for the Little-neck clam - Butter Clam - Horse Clam (*Protothaca staminea - Saxidomus giganteus - Tresus capax*) association is abundant within the Quinault marine shorelines. They tend to thrive in the high-energy zones where sandy beaches and pocket coves are found, especially where moderately sized rivers (such as Whale Creek, Raft River, and Duck Creek) are found, and provide local littoral cells filled with nutrient rich contributions. Within this association, the dominant edible species are large, relatively high yield, and are generally abundant (Schalk and Yesner 1988).

2.4.4. Fingered limpet-Sitka Periwinkle Association

The fingered limpet-Sitka periwinkle (*Acmaea digitalis-Littorina sitkana*) association is only found on near-shore habitats. Both the fingered limpet and the Sitka periwinkle species live within the intertidal zone, from the high zone (upper littoral zone) to the shallow subtidal zone.

Fingered limpets (Figure 14) attach themselves using pedal mucus and a foot. They move by flexing muscular contractions of their foot as they graze. They can "clamp down" to exposed rocky surfaces with considerable force and duration, enabling them to remain attached despite intense wave action.

The Sitka periwinkle is a small edible sea snail (gastropod) that breathes through gills. The limpet and periwinkle species, along with cohorts, tend to be only locally abundant within the near-shore habitats, but the overall distribution of this association is much wider than the razor clam associations (Schalk and Yesner 1988).

Figure 14. Fingered limpets and California mussels (Workman 2012).

2.4.5. Razor Clam - Bodega Clam Association

The area from Point Grenville south to Grays Harbor (North Beach of the CRLC) is home to the Razor Clam - Bodega Clam (*Siliqua patula - Tellina bodegensis*) association. The favorable habitat is low gradient sandy beaches, fully exposed to the surf. Razor clam habitat is found where their ability for rapid digging is facilitated by nutrient rich, sandy substrates. Although quantities of razor clams sufficient for commercial harvest occur at Kalaloch, Queets, Taholah, Raft River, and Hogsback, these are areas of minor production when compared to the North Beach CRLC (Schaefer 1939).

The remote ocean beaches of the pristine Olympic Peninsula are ideal razor clam habitat, which gives QIN harvesters, between Moclips River and Point Grenville, exclusive access to the densest razor clam resource on the Pacific Coast. Razor clams spawn within a period of a few days during May (Figure 15). Spawning is controlled by water temperature and begins when the temperature increases to approximately 55° F (Schaefer 1939).

Figure 15. Quinault razor clam bounty (Workman 2012).

2.4.6. Climate Change Impacts on Mollusk Populations

Strong evidence of global increases in atmospheric carbon dioxide (CO_2) concentrations have been observed and contribute to notable changes in the carbonate chemistry of ocean waters (Dore, et al. 2009, IPCC 2007, R. Feely, C. Sabine, et al. 2008, R. Feely, C. L. Sabine, et al. 2004). Elevated atmospheric CO_2 values are directly coupled with increased CO_2 oceanic concentration. This boost results in increased carbonic acid (H_2CO_3) and decreased pH values (reduction in oceanic pH). Recent hydrographic surveys and modeling studies have confirmed that the uptake of anthropogenic CO_2 by the oceans has resulted in a lowering of seawater pH by about 0.1 since the beginning of the industrial revolution (R. Feely, C. Sabine, et al. 2008).

Ocean acidification (dropping pH values) can result in environmental consequences, with physiological and ecological implications for marine organisms directly affecting the QIN. Shifts in oceanic pH values are of particular concern for species such as mollusks, coral reefs, pteropods, echinoderms (including starfish), and the larval stages of marine invertebrates that have calcium carbonate skeletons (Orr, et al. 2005, Kurihara 2008). In the Pacific Northwest Oceans, it is estimated that pH values have decreased by 0.08 units over the past 200 years (Orr, et al. 2005) and will continue to decrease at an annual rate of -0.0019 + 0.0002 pH units per year (Dore, et al. 2009).

The ocean is saturated with respect to calcium carbonate, but reduced ocean pH and carbonate ion concentrations will reduce the level of calcium carbonate saturation. Experimental evidence suggests that if these trends continue, key marine organisms, such as mollusks, corals, and some plankton, will have difficulty maintaining their external calcium carbonate shells (Orr, et al. 2005).

Recent oceanographic measurements demonstrate that acidified seawater is currently upwelling close to the Pacific continental shelf of the QIR (R. Feely, C. Sabine, et al. 2008) through vectors such as the Quinault Canyon. This acidified water may have adverse impacts on the larvae of native clams (such as the razor clam). The reaction in the Quinault Canyon of CO_2 with seawater reduces the availability of carbonate ions that are necessary for calcium carbonate ($CaCO_3$) skeleton and shell formation for marine organisms such as corals, marine plankton, and shellfish – including razor clams (R. Feely, C. Sabine, et al. 2008).

Chapter 3. Quinault Marine Coastline Factors of Influence

Relative Sea Level Change (RSLC) is expected to be seen along marine shorelines from the combined effects of global sea level rise and local factors such as vertical land deformation (e.g., tectonic movement, isostatic rebound[4]) and seasonal ocean elevation changes due to atmospheric circulation effects. In this document we review available projections of these factors for the marine waters of the Quinault Indian Reservation (QIR) and provide estimates of local RSLC for 2050 and 2100.

Based on the current science specific to the QIR, our "medium" estimate of 21st century RSLC is that very little RSLC will be apparent from the mouth of the Queets River south as far as Cape Elizabeth due to rates of local tectonic uplift that mostly offset projected rates of global sea level rise. Immediately south of Cape Elizabeth, in Taholah and extending southerly past Point Grenville, uplift is apparent in this region, but at rates lower than that observed on the northern coastline, with one notable exception centered at Kalaloch. The rates of RSLC along this coastline are not generally consistent between reaches.

3.1. Global Climate Change

The fourth Assessment Report of the Intergovernmental Panel on Climate Change (IPCC) projects general global sea level rise over the course of this century to be between 18 and 38 cm (7-15") for their lowest emissions scenario, and between 26 and 59 cm (10-23") for their highest emissions scenario. Relative Sea Level Change is the application of the changes in sea level with the anticipated changes in shoreline topography. Shorelines can rise or fall, independent of sea level, owing to the rebound of the land after the retreat of the glaciers, and from tectonic forces deforming the structure of the land (isostatic rebound).

The activities of people have been sending out emissions of carbon dioxide (CO_2), methane (CH), and nitrous oxide (N_20) through commercial activities causing the increase in global atmospheric levels of these compounds from the mid-19th century to the beginning of the 21st century by approximately 30%, 145%, and 15% respectively (Houghton, et al. 1995). Atmospheric levels of carbon dioxide have increased over the same period from an estimated 280 parts per million by volume (ppmv) (Bolin, et al. 1977) to present day levels of approximately 360 ppmv (Houghton, et al. 1995). Higher concentrations of greenhouse gasses reduce the ability of the Earth to radiate planetary heat through the atmosphere and have resulted in a trend of global climate warming (Houghton, et al. 1995, IPCC 2007).

Terrestrial and aquatic plants withdraw carbon dioxide from the atmosphere in the process of photosynthesis (Vygodskaya, et al. 1997). Carbon sequestered from the atmosphere is stored in plant fiber (above and below ground) for extended periods of time, especially in perennial plants such as trees (Bolin, et al. 1977, IPCC 2007, Houghton, et al. 1995, Schlosser, Bassman and Wagner, et al. 2002). Higher atmospheric carbon dioxide levels, combined with increased atmospheric nitrous oxide contribute to enhanced plant productivity generally and, consequently, to the rate at which carbon dioxide is removed from the atmosphere (Burton

---

[4] Isostatic Rebound: An expression of the landform effects of vertical crustal motion, local and global sea level changes, local and regional horizontal crustal motion, gravity field adjustments, and tectonic plate stresses leading to earthquakes. Studies of isostatic rebound provide information about the movement of mantle rocks and the impacts of past ice sheet history. These are important to the study of mantle convection, plate tectonics, the thermal evolution of the Earth, glaciology, paleoclimate and changes in global sea level changes.

1997, Schlosser, Bassman and Wandschneider, et al. 2003). The magnitude of these combined processes remains largely undetermined. However, it is clear that terrestrial and aquatic ecosystems have been unable to offset increased emissions of carbon dioxide from the burning of fossil fuels, forest fires, and other sources as evidenced by raising atmospheric carbon dioxide levels (Schlosser, Bassman and Wandschneider, et al. 2003).

The earth's climatic cycles (Figure 16) show that we are still in the process of leaving the last Ice Age. The climate is in a warming process and the impact of increased greenhouse gas emissions on climate change is best expressed by asking if these emissions are speeding the warming cycle of our planet at a dangerous rate.

3.2. Glaciation in the Olympic Mountains

About 12,000 years ago vast Olympic Peninsula glaciers were in retreat, leaving behind rounded valleys and marshy meadows. Elk, bison, wolves and mastodons roamed the land, and humans roamed with them (NPS 2009).

The American mastodon (*Mammut americanum*) lived in this region of North America. Mastodons are thought to have first appeared almost four million years ago and became extinct about 10,000 years ago, at the same time as most other Pleistocene megafauna. Though their habitat spanned a large territory, mastodons were most common in ice age spruce forests within and around the QIR (Crystal 2010). During the Pleistocene Epoch, 1.6 million to 10,000 years ago, much of North America was covered by great sheets of ice (Scotese 2002).

A partial skeleton of a mastodon was recovered within a thick deposit of "blue" lake clays along the lower Quinault River. Current research into the date of these and similar clay units along the outer Washington coast suggests a non-glacial interval age (~20,000–60,000 years before present) for this find (Thackray 1996).

On August 22, 1928, a tusk from wooly mammoth was found on the Quinault River. Then on January 17, 1929, a wooly mammoth fossil was found 3½ miles below Lake Quinault on the Quinault River (Workman 2010). By February, 1930, more bones were unearthed in an ancient wooly mammoth wallow on the lower Quinault River. Again on January 21, 1956, a six foot long pre-historic wooly mammoth tusk was found north of Hoquiam, on the west side of US101 (Workman 2010). On January 12, 1992, mammoth ivory was unearthed by a big landslide along the Quinault River.

In 1977 a farmer near Sequim, WA, digging a pond, unearthed remains of a mammoth. Embedded in one of the animal's ribs was a broken piece of antler or bone resembling a spear point. The spear point, and other signs of human occupation, are the earliest evidence of human presence in this region, and proof that Olympic Peninsula inhabitants 12,000 years ago were hunters (NPS 2009).

By about 3,000 years ago, as the aboriginal human population increased, early inhabitants shifted their focus to lowland rivers and lakes. Fishing, gathering shellfish, hunting sea mammals and land mammals formed the foundation of a rich and complex culture (NPS 2009).

Global climate is highly variable and currently is in a cycle of warming because we are still leaving the last Ice Age of the Pleistocene Epoch (Figure 16) and because of the anthropogenic additions of greenhouse gases to the atmosphere (Scotese 2002). This cycle of global climate change holds the potential to disproportionately impact coastal populations.

Global warming causes sea level to rise as terrestrial ice melts, oceans expand, and storm patterns become more energetic (FMI 2008). Consequently, it affects most of the world's coastlines through inundation and increased shoreline erosion. Accurate predictions of the development of these effects over the next century are needed in order to manage the resulting risks. Coastal flooding is somewhat easier to predict than erosion since inundation can generally be estimated using coastal elevation contours (FMI 2008). However its prediction is not trivial since inundation may be followed by rapid reshaping of the shoreline by, amongst other things, waves, tidal currents and human interventions.

Global warming occurred rapidly at 10,000 years ago, but was later followed by several cooler periods. Another milder warming, known as the Medieval Optimum, occurred from 1100 to 1300. During the Little Ice Age of 1450 to 1890, many glaciers in the Olympics, such as the Anderson Glacier, extended or re-established in their basins. The warming trend since the late 1800s has caused the complete melting of this last remnant of the Little Ice Age.

3.2.1. Olympic Glacial History: western slopes

The Olympic Mountains are glaciated by alpine glaciers. The glaciers are mainly cirque glaciers, but a few valley glaciers are also present along the western slopes where precipitation is greatest (such as in the Quinault River and

Figure 16. During the last 2 billion years the Earth's climate has alternated between a frigid "Ice House" and a steaming "Hot House" (Scotese 2002).

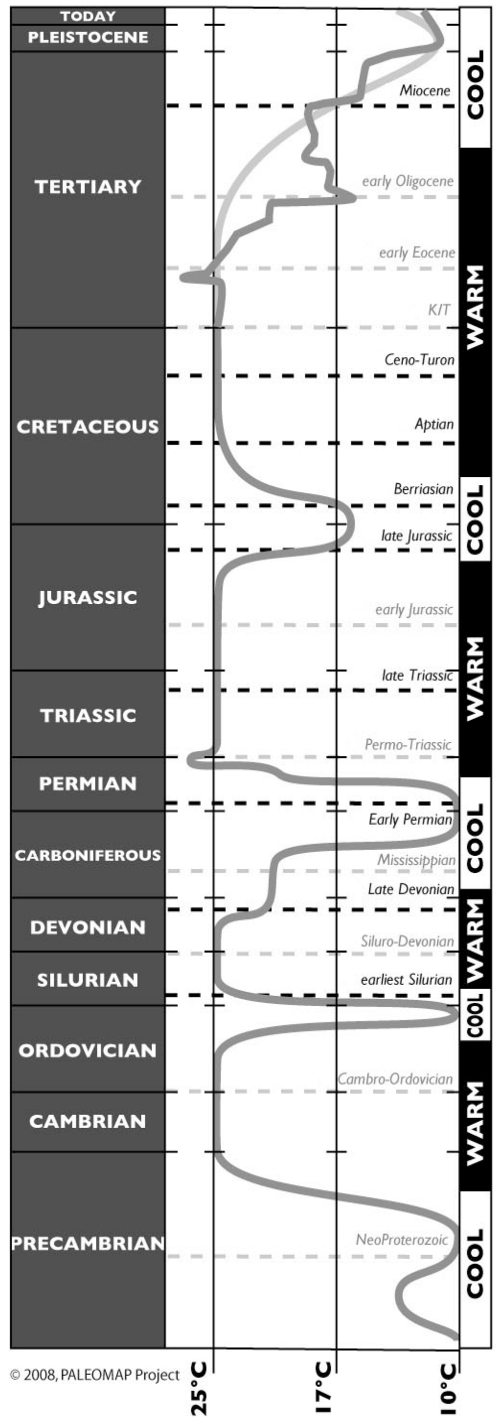

Queets River drainages). During the last major glacial episode, the Cordilleran Ice Sheet from the northern Coast Range and Fraser Lowlands of British Columbia, Canada, reached the eastern and northern sides of the Olympic Mountain range through the Strait of Juan de Fuca and Puget Sound lowlands (Figure 17). These glacial events did not glaciate the Olympic Mountains.

Figure 17. Paleogeography (Burke Museum 2012) showing the glacial ice cap over western North America during the last ice age.

The Olympic Mountain glacial maxima were reached during the Quaternary Period (Figure 2) when glaciers of the Olympic Mountains reached their zenith and eroded through extensive valley glaciers (Crandell 1965, Thorson 1980). The Olympic Mountain alpine glaciers began their retreat around 15,000 years ago and continued that retreat through about 12,000 years ago. Since that time, the rate of retreat within the Olympic Mountains has substantially slowed although many glacial units have recently diminished in size to cross the threshold of viable glacial process contributors (e.g., Anderson Glacier). The coastline has been transient as sea levels moved up and down, and the land resources vertically retreated or advanced (isostatic rebound and compression), all expressed as (RSLC) (McCroy, et al. 2002).

The Quaternary history of the glacial advances for both the Cordilleran Ice Sheet and alpine glaciers has been examined in the Olympic Mountains by Hellwig (2010). That study of glacial events through the Quaternary Period provided an extensive review of glacial progression and the potential effects of climate change on the network of glaciers. Data reported in this section (Section 3.2.1, Olympic Glacial History: western slopes) comes greatly from that graduate study effort.

While the Cordilleran Ice Sheet dissipated nearly 20,000 years ago, the Olympic Mountain alpine glaciers still endured (Spicer 1989). The Olympic Mountain glacial complex developed into large valley glaciers that advanced and retreated with climatic fluctuations. These glaciers formed a large snow and ice complex from which the valley glaciers drained (Crandell 1964, Spicer 1989). The glaciers of the western and southern sides of the Olympic Mountains drained onto the coastal plain of the southwestern Olympic Peninsula and merged to become broad piedmont lobes close to, or at, sea level (Crandell 1965, Speicer 1986). Moraines mark the furthest extent of the valley glaciers in the river valleys such as those seen in the Quinault River valley between Taholah and Amanda Park.

The western side of the Olympic Mountains had no continental ice sheet interacting with the alpine valley glaciers making it possible to interpret their glacial extent. Thackray (2001) discovered that the alpine glaciers in the Olympic Mountains descended into the valleys and coastal lowlands six times during the late Wisconsin Glaciation and deposited extensive geomorphic features and a stratigraphic record that contains abundant organic material. The Quinault, Queets, and Hoh River Valleys were examined as they had large glaciers repeatedly descend through them to the coastal plain, erode material, and deposit thick sediment layers and landforms. Postglacial shoreline erosion and fluvial incision have exposed both the glacial and non-glacial sedimentary sequences in stream cuts and sea cliffs in these river valleys. Each glacial advance (followed by a glacial retreat), consists of a thick outwash layer and a thin layer of ablation (processes that remove snow, ice, or water from a glacier), or lodgement till (materials compacted under the weight of the glacial formation then exposed after glacial retreat), with thick post-glacial lake sediments appearing up-valley from end moraine dams. The locations of the last glacial maximum ice margin in the Hoh, Queets, and Quinault Valleys have been established through the mapping and dating of glacial deposits, such as drumlins, glacial valleys, and terminal moraine features (Thackray, Extensive Early and Middle Wisconsin Glaciation on the Western Olympic Peninsula, Washington, and the Variability of Pacific Moisture Delivery to the Northwestern United States 2001).

3.2.2. Glacial Load and Isostatic Rebound

Since the retreat of the last glacial period on the Olympic Mountains (about 12,000 years ago), the region has been showing response to isostatic rebound of the terrain. This started when the heavy ice sheets of the repeated glacial periods (Pleistocene Epoch, Figure 16) compressed the landforms down, depressing the earth's crust into the mantle below. As this happened, the absolute altitude of the landforms lowered under the weight, and sea levels dropped because water was being retained in glaciers around the world. In relative terms, the lowering of sea level was faster than the decompression of the mantle in this region, and RSLC was witnessed as lowering sea levels and lowering land forms. The marine shorelines of the Quinault Coastline existed far to the west of the current location.

As the glaciers melted, and retreated, the mantle started the slow and steady process of rebounding by flowing back to its original position. At the same time, sea levels started to climb as more terrestrial water was cycled through the clouds, to land as rain and snow, melted into rivers, entered the oceans, and then evaporated again to the clouds as part of the natural water cycle. This post-glaciation cycle has been unfolding for well over 11,000 years in this pattern of response.

Some have maintained that this isostatic rebound is amplified by the changes in overburden of the land caused by the harvest of old growth timber within the region during the past 100 years. Although the weight of the old growth timber is minor when compared to the weight of thick glaciers, it is not inconsequential. More important, the timber was not present during the glaciation events so its addition may have served to slow the rate of isostatic rebound while its release may discharge the terrain to continue the rebound process.

As the glaciers on the Olympic Peninsula receded, the land structure has rebounded from the loss of ice sheet weight. This load of ice was a substantial burden on the land, and as the glaciers formed, the response was to see the land depressed beneath the ice sheet and become slightly elevated outside the ice sheet owing to mantle flow (Figure 18). During deglaciation the depressed region rises and peripheral regions subside. Uplift of the Earth's surface is frequently observed as dropping RSLC in recently deglaciated areas.

Figure 18. During glaciation (a). During deglaciation (b).

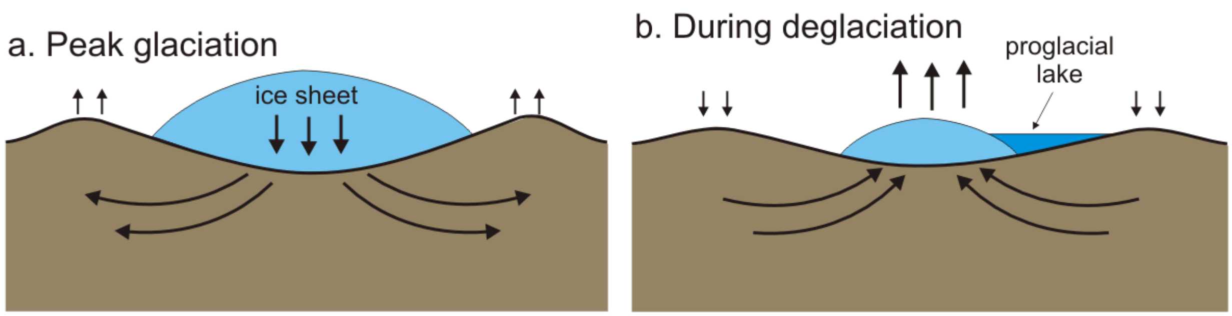

Relative Sea Level Change is affected by the melting of glaciers in two important ways:

1. Glacial meltwater changes global sea level by increasing the volume of water in the oceans, and
2. Vertical movement of the land associated with the Earth's response to unloading produces a local apparent change in sea level.

The ongoing uplift and tilting of QIR lands caused by postglacial rebound affects local sea level and, consequently, shoreline erosion (Pazzaglia and Brandon 2001). River flow is also affected through changes in stream bed gradients and the elevation of lake outlets. Global climate change studies related to issues of changing sea level arise quite naturally from postglacial rebound, as it is primarily the changing mass balance of glaciers and ice sheets that affect global sea level.

The western coastal range of the Olympics studies by Thackray (1999) have revealed several insightful findings of isostatic uplift (post-glacial rebound) and lowering (Figure 19). The findings indicate a syncline epicenter (area of acute land lowering) located near Kalaloch that extends southerly to near Queets. Lands beyond the syncline have responded with substantial rebound. These estimates of Thackray were combined with findings showing rebound to the crest of the Olympic Mountains by Hellwig (2010). When viewed together (Figure 19), the isostatic-uplift rates show a significant response to the deglaciation of the region. These uplift rates represent only the rebound of the land and do not include the rate of sea-level rise associated with the post-glacial period.

According to Thackray, the Kalaloch syncline is a broad (>32 km, 20 mi, wavelength), low-amplitude fold deforming the Pleistocene glacial-nonglacial stratigraphic sequence. The elevation pattern of the wave-cut surface expresses the syncline most clearly. Geological uplift rates range from −0.03 to 0.7 mm/year. The simultaneous uplift of certain areas combined with the seismic drop of adjacent areas leads to interseismic strain accumulation. These areas can respond with stress-relieving motion instigated by an earthquake in the area. In other cases, the pressures can lead to earthquake events as pressures are relived.

Postglacial rebound is seen in response to changes in the cover of lands impacted by glacial inundation. The surface load caused by the Olympic Mountain-scale glaciers of the last ice age depressed the surface of the Earth. With the decay and retreat of the ice sheets the depressed areas began to rise toward their former position. Postglacial rebound doesn't happen instantly because at great depths the Earth acts like a thick, viscous fluid with a delayed response.

Holdahl, Faucher and Dragert (1989) suggested the northwest Olympic Peninsula (on the Makah Indian Reservation) was rising approximately 2 mm/yr (net decrease in RSLC). Other recent analyses (Verdonck 2006) support the conclusion of general uplift occurring along most of the outer coast with the greatest uplift (>3mm/yr) located in the northwest corner of the Olympic Peninsula. Hellwig (2010) determined the rebound along the western edges of the Olympic Mountain crest (>2mm/yr) where the largest glaciers were established the longest (Figure 19). Verdonck (2006) recalculated RSLC and again found some strong local subsidence (net increase in RSLC) on the central Washington coast (near Kalaloch).

Ongoing GPS measurements at Pacific Beach, WA, suggest uplift in this region of the outer coast of 1.8 mm/yr (Mote, et al. 2008). Reliable estimates of sea level change for the central and southern Washington coast are not available due to sparse data, but are estimated to be on the order of 0-2 mm/yr of geologic uplift. These estimates are made from measurements of the single factor of net sea level change, without accounting for tectonic factors, or climate change, changing sea level, or water temperatures. All of these factors, and others, combine to generate the net effect of RSLC on the QIR marine shorelines.

Relative sea level has passed through four general stages since the late Pleistocene. The first stage associated with deglaciation (13,000-11,000 yr before present (B.P.)) was a rapid planetary (eustatic) rise in relative sea level. Between about 11,000 and 9,250 yr B.P., isostatic rebound (locally to the Olympic Peninsula) resulted in a rapid drop in relative sea level. Continued eustatic sea level rise after 7,000 yr B.P. produced submergence of shorelines until about 4,500 yr B.P. Both isostatic and eustatic forces were attenuated during the last 4,500 years when tectonic factors became the major determinant of late Holocene sea levels. Sea level during the late Holocene epoch (post Pleistocene epoch) was divergent for the eastern and western sides of the Olympic Peninsula with submergence the general trend for the eastern side and emergence for the western. It must be emphasized that this description is based largely on extrapolation from historic geodetic and tide-gauge measurements or from prehistoric relative sea level records of surrounding areas. Data on relative sea level for the Olympic Peninsula are poor and as more information is acquired, the model proposed here may prove to be far too simplified (Burke Museum 2012, Crandell 1964, Glick, Clough and Nunley 2007, Hellwig 2010).

Figure 19. Tectonic isostatic rebound showing land deformation, adapted from Hellwig (2010) and Thackray (1999). Contours used adaptation from Holdahl *et al.* (1989), with 1.2 mm added to account for eustatic sea-level rise.

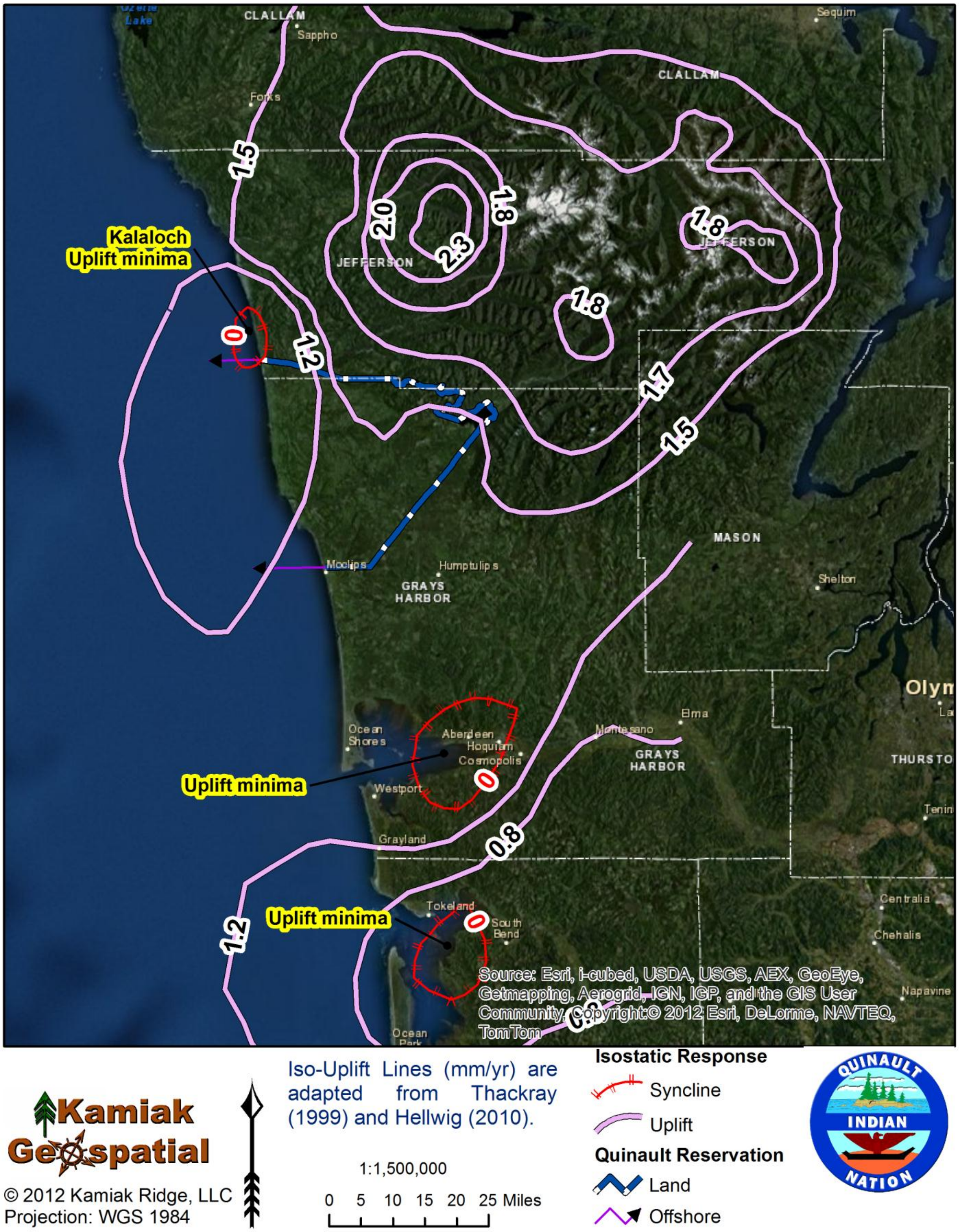

3.1. Temperature & Precipitation

There is a high degree of weather variability within the QIR. Topographic variations that begin at sea level are influenced by the rising hillsides that climb to the peaks of the Olympic Mountains east of the QIR. Stream networks that traverse the QIR are fed by a combination of foothill and mountain ridge sources. Precipitation is highly variable and shows tendencies of increasing precipitation with increasing elevation (Figure 21).

Data for this report concerning monthly weather trends within the QIR were created using the PRISM (Parameter-elevation Regressions on Independent Slopes Model) climate mapping system, developed by Dr. Christopher Daly, PRISM Climate Group director at Oregon State University. PRISM is a unique knowledge-based system that uses point measurements of precipitation, temperature, and other climatic factors to produce continuous, digital grid estimates of monthly, yearly, and event-based climatic parameters. Continuously updated, this unique analytical tool incorporates point data, a digital elevation model, and expert knowledge of complex climatic extremes, including rain shadows, coastal effects, and temperature inversions. PRISM data sets are recognized world-wide as the highest-quality spatial climate data sets currently available. PRISM is the USDA's official climatological data (PRISM Climate Group 2012).

PRISM is an analytical model that uses point data and an underlying grid such as a digital elevation model (DEM) for a 30 year climatological average (e.g. 1981-2010 average) to generate gridded estimates of monthly and annual precipitation and temperature (as well as other climatic parameters). PRISM is well suited to regions with mountainous terrain, because it incorporates a conceptual framework that addresses the spatial scale and pattern of orographic processes. Grids are modeled on a monthly basis. Annual grids of temperature are produced by summing the monthly grids (PRISM Climate Group 2012).

3.1.1. Precipitation

Within the Olympic Mountain influence area, winter storms generally bring moisture travelling from the southwest to the northeast (Figure 20), and are uplifted by the terrain, creating a precipitation maximum on the windward side and a minimum on the leeward side (Figure 21) (Mass 2008).

Figure 20. Direction of Weather System flow bringing rains to the Olympic Mountains and Western Washington (Mass 2008, PRISM Climate Group 2012).

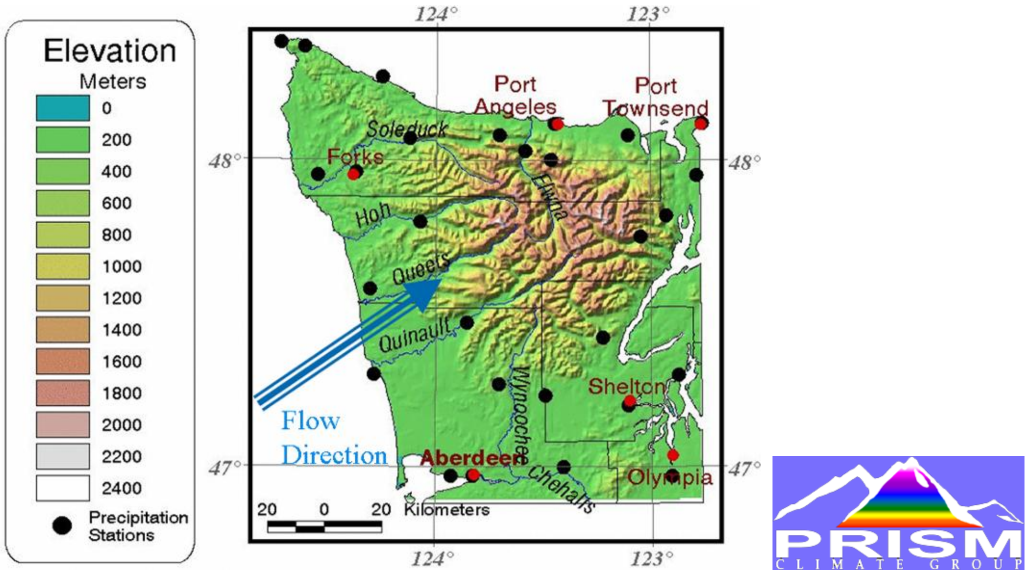

Figure 21. Precipitation distribution within the Olympic Peninsula showing the comparative high precipitation amounts along the western coastline, lower amounts within the Puget Sound area (rain shadow effect), and the maximum precipitation amounts along the Olympic Mountain crest (PRISM Climate Group 2012).

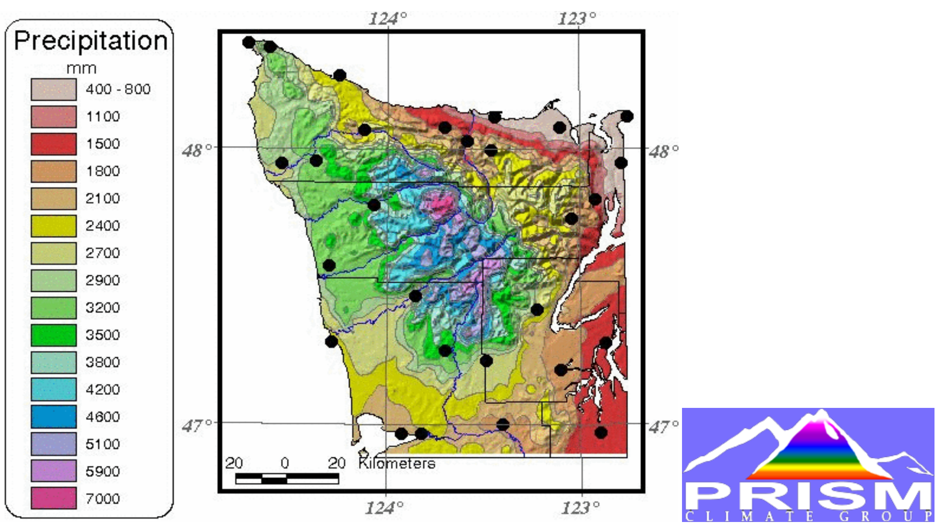

These weather patterns bring a variable weather model to the QIR. Precipitation shows monthly variations that are responsive to the topography of the QIR with the lowest annual precipitation amount (85 inches per year) seen along the ocean shoreline at Point Grenville (NOAA 2011). This pattern yields to the uplift provided by the terrain to witness the highest precipitation amounts northwest of Lake Quinault, where totals reach 165 inches per year (Figure 22) (PRISM Climate Group 2012).

Figure 22. Annual Precipitation derived from PRISM datasets from 1980-2010 on the QIR (PRISM Climate Group 2012).

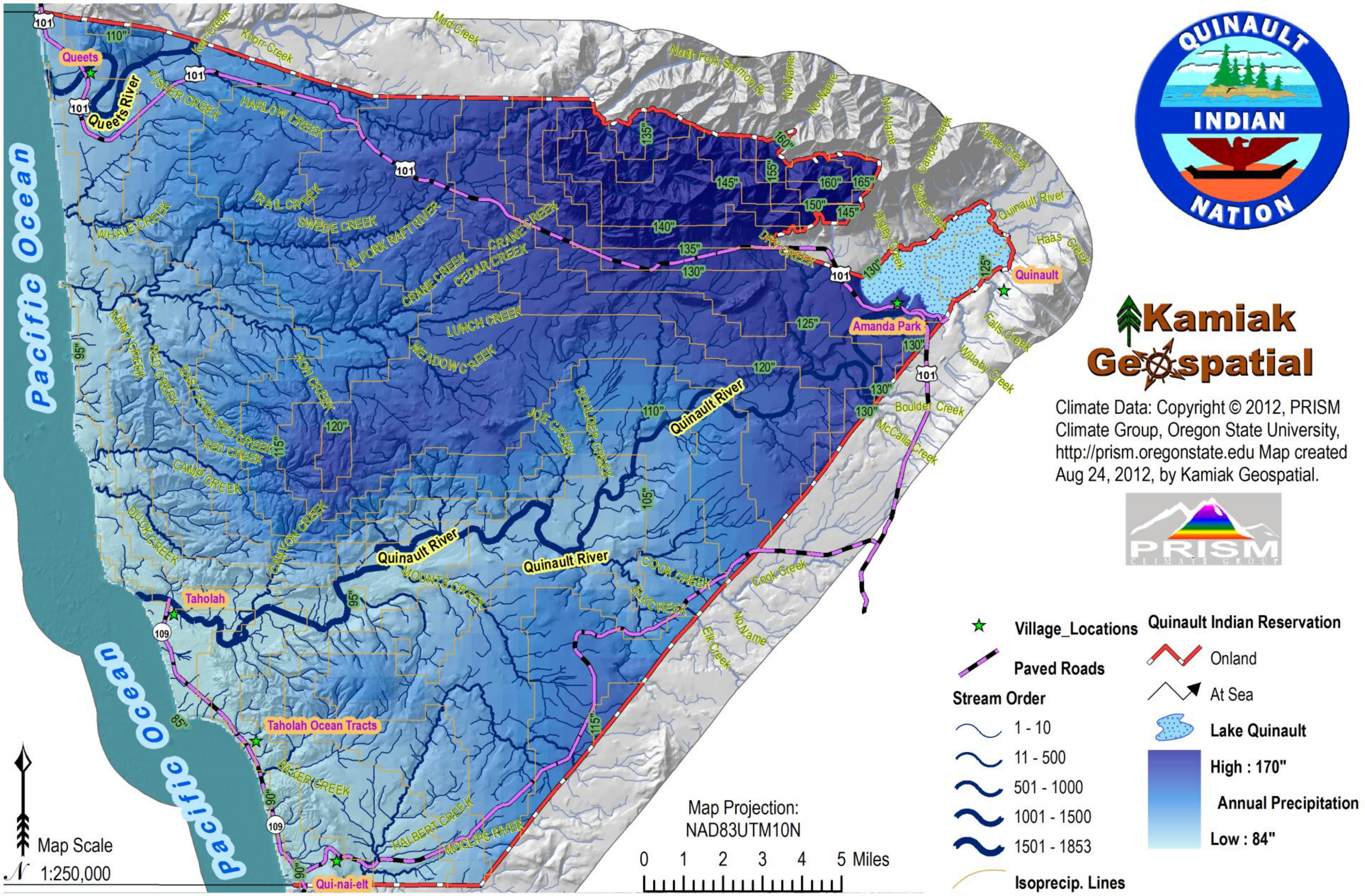

The timing of precipitation events within the QIR is responsive to the seasons of the year. The months receiving the highest amount of precipitation include October through March when approximately 77% of annual precipitation arrives (Table 2). These reported values represent an average precipitation amount across the entire QIR, not just selected extreme precipitation locations (where higher and lower amounts can fall with every storm).

Table 2. Average Monthly Precipitation for all of the QIR (PRISM Climate Group 2012).

Month	Average Monthly Precipitation (inches)	Percent of Total
Jan	16.5	15%
Feb	11.9	11%
Mar	11.6	10%
Apr	8.6	8%
May	5.4	5%
Jun	4.0	4%
Jul	2.2	2%
Aug	2.5	2%
Sep	3.9	3%
Oct	10.7	10%
Nov	19.2	17%
Dec	15.4	14%
Total	112.0	

The deviation within the QIR between the areas receiving the highest precipitation and the lowest precipitation is striking. The heavy November showers can deposit almost 35 inches of rainfall in the North Boundary area while at the same time the region from Taholah to Moclips may only receive 13 inches in November (Figure 23).

Figure 23. Monthly precipitation showing the average normal precipitation on the QIR, as well as maximum and minimum precipitation (PRISM Climate Group 2012).

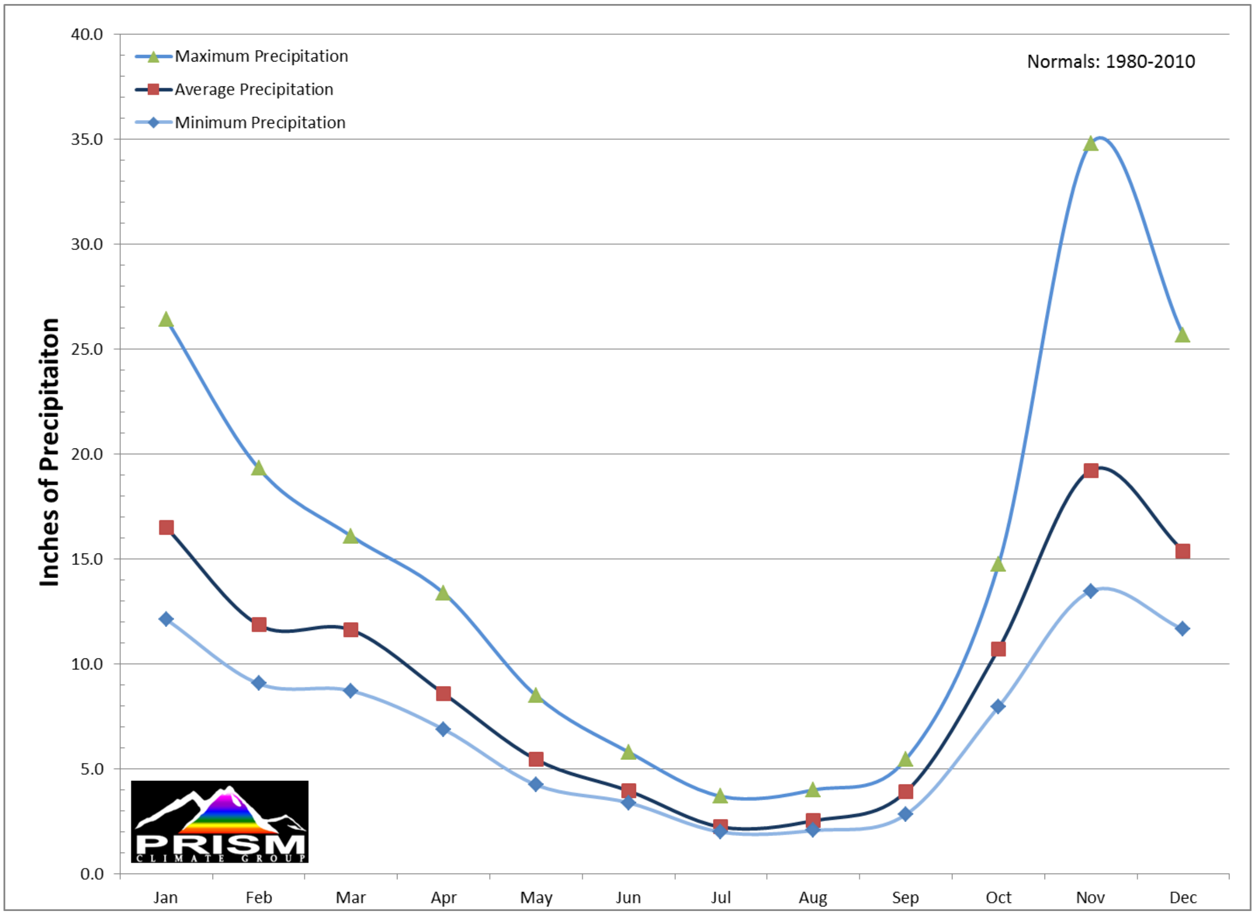

3.1.2. Temperature

Temperature is equally variable in response to topographic lift and the presence of the Pacific Ocean as a moderating force keeping the adjacent lands cool in the summer and relatively warm in the winter. The average monthly hottest temperatures on the QIR are observed in August when the thermometer can climb to an average high temperature of 75º F in Amanda Park while that same average monthly high is only 62º F in Taholah (Figure 24). That is not to say that the temperature on the QIR does not exceed these values. The determination of the highest average temperature is completed by recording the high temperature each day of the month at observation points and then creating an average temperature based on those values.

Conversely, the coolest month of the year on the QIR is generally seen as January when the average monthly low temperature reaches only 30º F along the upper elevations of the North Boundary to the northwest of Amanda Park. At the same time, average monthly low temperatures in Taholah will moderate to only 35º F (Figure 25). The determination of these monthly low-averages is determined much like the average high temperatures. In this case, the lowest daily temperatures are recorded each day of the month at each recording station and then averaged to determine the average low temperature across the QIR (PRISM Climate Group 2012).

Figure 24. August average high temperatures on the QIN, the “hottest month of the year” (PRISM Climate Group 2012).

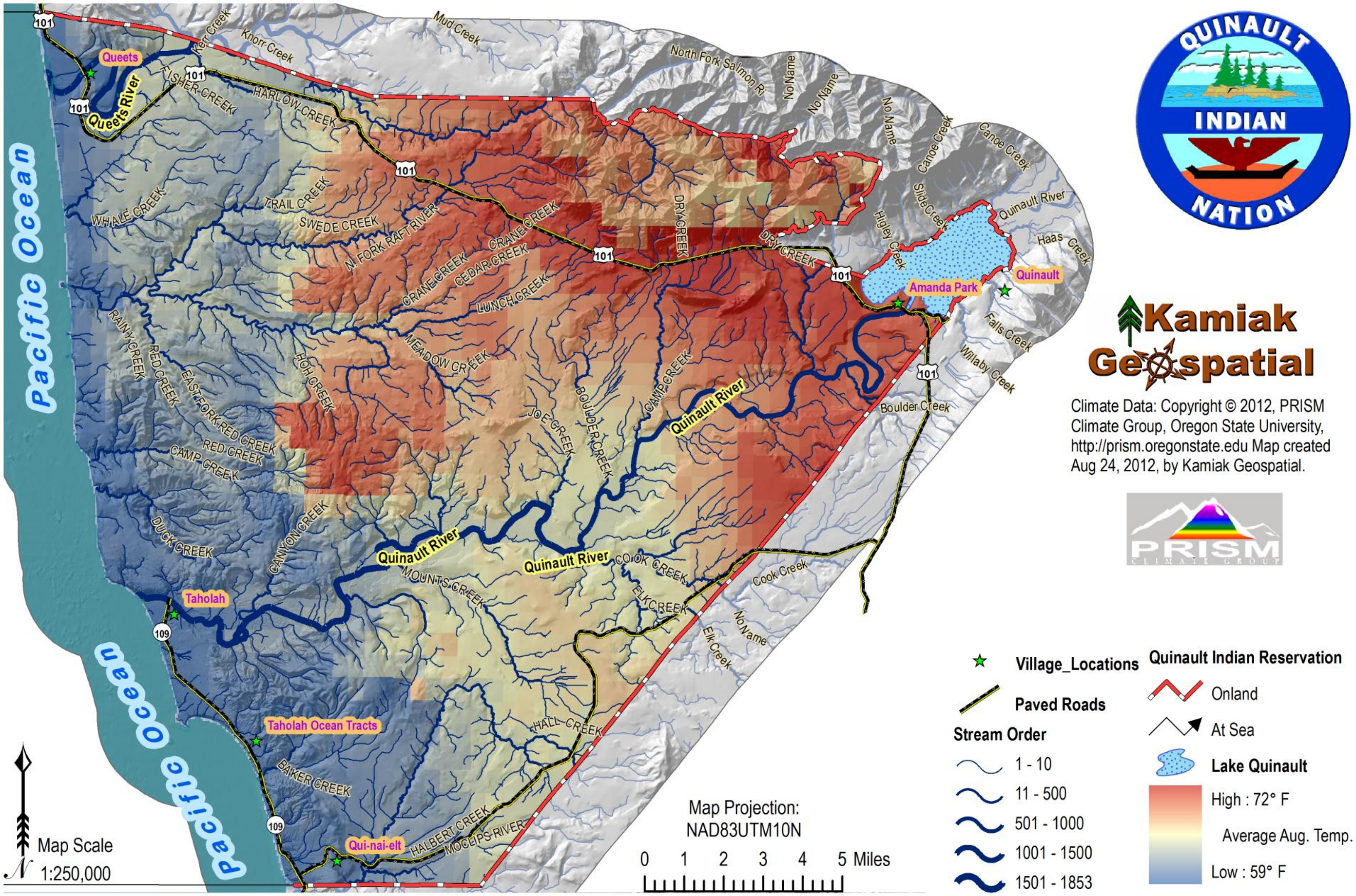

Figure 25. January average low temperatures on the QIN, the "coldest month of the year" (PRISM Climate Group 2012).

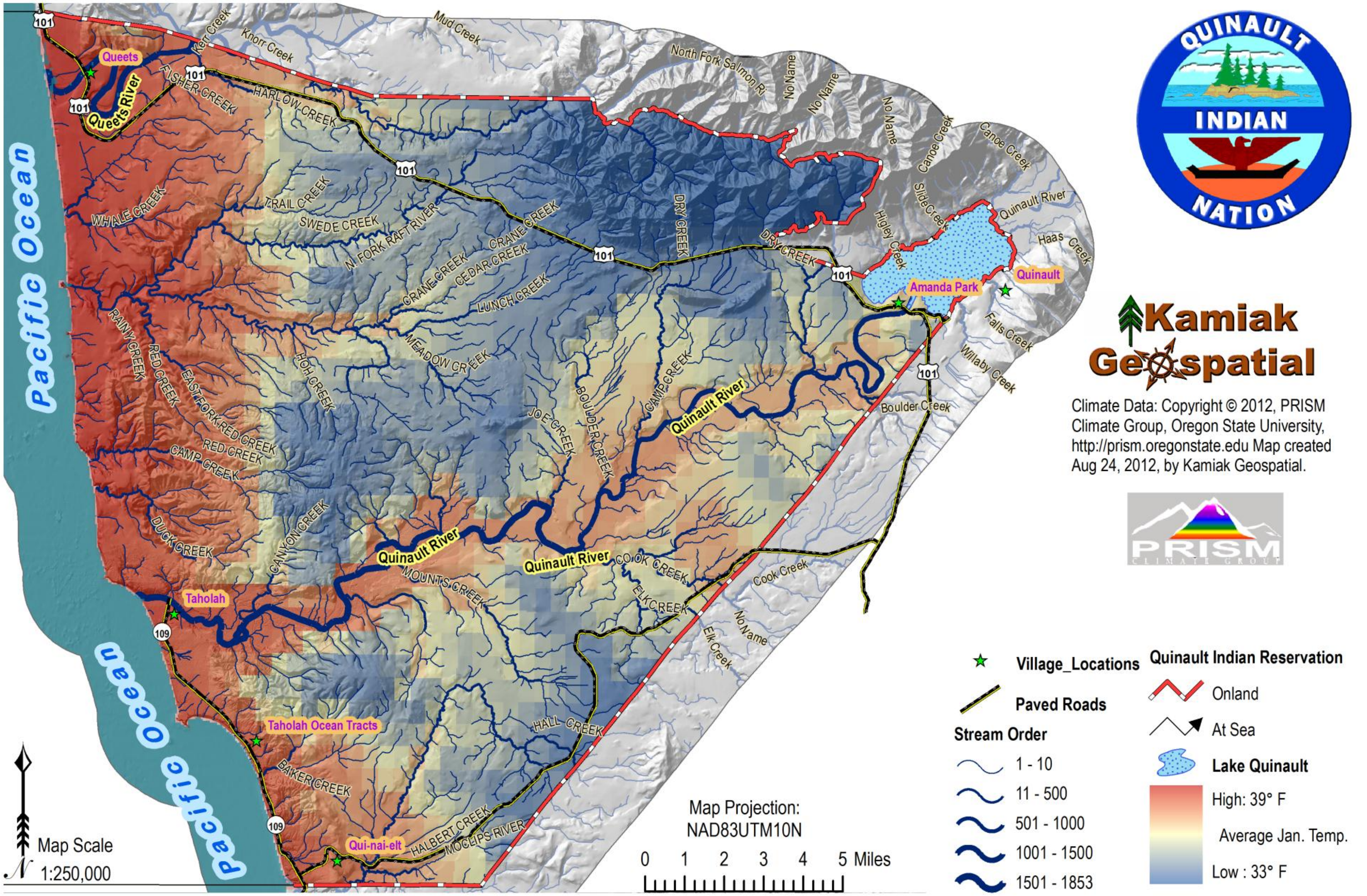

Monthly temperature extremes reveal that the variation from the highest average monthly temperature in a selected month may differ from the lowest average monthly temperature on the QIR by as much as 26º F in July and August (Table 3).

Table 3. Variations in Monthly Temperature within the QIR (PRISM Climate Group 2012).

	Lowest Monthly Temperature (º F)		Highest Monthly Temperature (º F)	
Month	**Minimum Lowest Monthly Temperature**	**Average Lowest Monthly Temperature**	**Average Highest Monthly Temperature**	**Highest Maximum Monthly Temperature**
Jan	30.1	33.8	44.9	46.5
Feb	31.5	34.6	48.4	49.5
Mar	32.2	35.5	51.8	52.4
Apr	35.0	38.1	56.3	58.6
May	40.0	42.6	61.7	65.4
Jun	45.2	47.0	65.5	69.6
Jul	49.0	49.8	69.9	75.5
Aug	49.3	50.3	70.6	75.3
Sep	46.8	47.4	68.3	71.0
Oct	41.6	42.4	59.9	61.6
Nov	35.4	37.5	50.3	52.0
Dec	31.9	34.7	45.4	46.9

While precipitation across the QIR was presented to show the differences in monthly amounts, the same can be presented for temperature (Figure 26). The warmest temperatures seen on the QIR (Figure 24) exhibit the greatest variation during the period May through September (Table 3, Figure 26), when the difference between the average high temperature and the highest temperatures is about 5º F. The difference between the coolest and warmest places on the QIR can be as much as 25º F during August (lowest average low to the highest average high). These characteristics define the temperate ecotype known to this region that combine moderated temperatures (few extreme lows and few extreme highs) with frequent and high amounts of precipitation delivered every month of the year.

Figure 26. Temperatures showing the average temperature between the warmest and the coolest months on the QIR (PRISM Climate Group 2012).

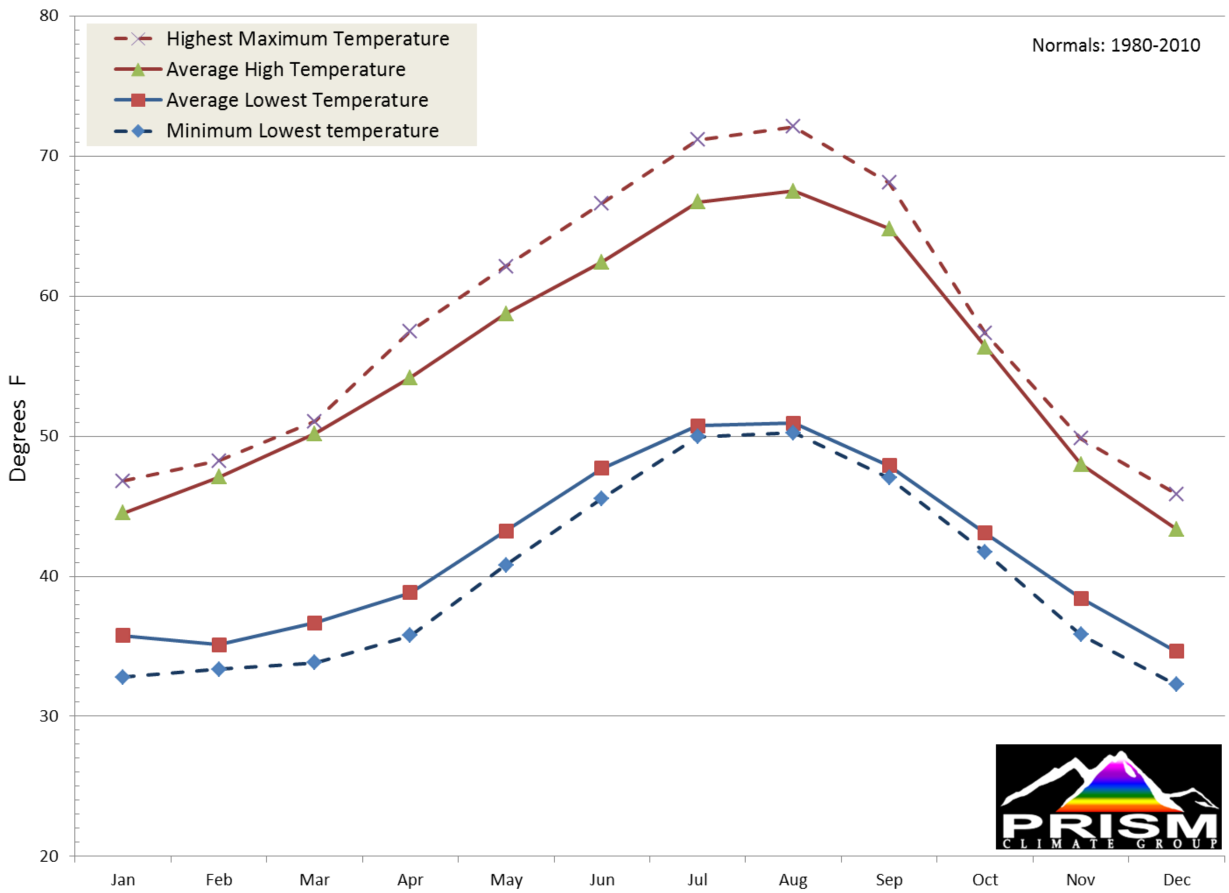

Clouds and precipitation are greatly enhanced when air is forced to ascend the windward slopes of mountain barriers. An extensive region of light to moderate precipitation linked to a strong Pacific low-pressure system and its associated fronts can bring significant precipitation to the region. This precipitation is then greatly increased, sometimes by factors of two to five times, as air ascends the mountains (Mass 2008).

3.1.3. Weather Change Impacts

Predictions of Global Climate Change influences for this region are anticipated to be seen as deviations in temperature and precipitation patterns, and the resulting changes to river flow rates, water temperatures, and oceanic wave forms. One of the most striking, and predictable, is the impact expected to be seen across the Olympic Mountains as glaciers continue to diminish in size and even expatriate from the peaks of the mountains (such as has been recently observed at Andersen Glacier at the headwaters of the Quinault River – Death of a Glacier (Workman 2012)).

Recent history demonstrated by the PRISM models (PRISM Climate Group 2012) show how temperatures within the QIR are expected to rise during the coldest months of winter and moderate in the late fall period as precipitation increases in the pre-winter periods. This may lead to diminished snowfall at the peaks of the mountains, reduced glacial formation, and increased winter-time river flow rates.

Taken to the next level of analysis, this could signal dewatering events (periods of time when water flow ceases and stagnates in the riverbed) within the major river systems of the QIR during the warm summer months. The Quinault River and Queets River both rely on glacial melt delivered to the rivers as hyporheic (subsurface) flow and surface water flow (Schlosser, Armstrong and Schlosser 2011).

The hyporheic zone is a region beneath and lateral to a stream bed, where there is mixing of shallow groundwater and surface water. The flow dynamics and behavior in this zone (termed hyporheic flow) is recognized to be important for surface water/groundwater interactions, as well as fish spawning, among other processes (Orghidan 1959).

The flow dynamics in the Quinault River are controlled by the pressure variabilities arising on the stream-bed when the flowing water is diverted by stream-bed irregularities created by benthic fauna, moving sand dunes and other obstacles (Schlosser, Armstrong and Schlosser 2011). The mechanism of hyporheic flow can be triggered also by groundwater upwelling seepage beneath the stream-bed and alongside the stream banks.

These water contributions (including glacial contributions), are released into the soils and ultimately into the streams through hyporheic flow mechanisms. These contributions have kept the rivers flowing year-round with a low probability of dewatering events. These waters also deliver nutrient rich particles available to fish. With the so called “death of the glaciers”, this contribution of “dry-season” water to the river systems is forfeited and the flow rates through the rivers in the hot and dry summer months are decreased.

Although much of the interest in this document, and others, has focused on the Global Climate Change effects on marine shorelines, the river processes feeding the marine shorelines has far-reaching impacts. The variety of salmon species returning to their natal streambeds for spawning is key to triggering the secondary and tertiary effects seen downriver, at the mouth of the rivers, and offshore into the ocean.

Warming of the climate and increases to wintertime rainfall (as opposed to wintertime snowfall), will witness higher wintertime river flow rates and increasing riverbed erosion from increased peak flow. Consequentially, the summertime flow rates may be reduced as hyporheic flow and surface water flow rates are diminished (because of the reduction in glacial and snow melt). In time, the impacts of Global Climate Change will lead to substantial alterations of fish populations returning to QIR rivers. As these changes are witnessed, the consequent impacts to marine mammals and mollusks will follow.

Those impacts to secondary species may take centuries to witness, but the impacts to fish species is expected to be seen first, and may be witnessed within the next century. Some of these impacts may have already been initiated as efforts are underway to mitigate the loss of specific salmon species habitat (e.g., blueback salmon habitat restoration in the Upper Quinault River (Schlosser, Armstrong and Schlosser 2011)).

Chapter 4. Coastline Response to Accelerated Sea Level Change

The most widely cited method of quantifying the response of a shore to rising sea levels is known as Bruun's rule (Davis 2005). This was developed to describe the behavior of sandy coasts with no cliff or shore platform. It assumes that the wave climate is steady and consequently the beach profile (average equilibrium) does not change, but does translate up with the sea level. This rise in beach surface requires sand, which is assumed to be eroded from the upper beach and deposited on the lower beach (Davis 2005). Thus, as the profile rises with sea level it also translates landward, causing shoreline retreat. These shoreline prediction responses do not adequately reflect the sandy beach to rocky cliffs topography found across the QIR ocean shoreline. The ocean shorelines in the southern reaches of the QIR, for instance at Moclips River and Wreck Creek, are different than the cliffs at nearby Cape Elizabeth (Figure 27). These are different in composition to the shorelines at Pratt Cliff or Hogsback, Queets, or Duck Creek (Figure 28), piercement structures (Figure 29), Raft River, or any of a hundred other locations along the QIR ocean shoreline.

Another constraint on the range of applicability of the Bruun rule results from its assumptions that the shore profile is entirely beach and loses no sediment. The QIR coastlines is made from surface deposits that can only be eroded a limited amount before the land underlying it is exposed and degraded. The QIR shore profiles are composed of beach sediments, conglomerate materials, seafloor sediments, and rock. The rock element of such composite shores complicates its behavior because it can only erode (not accrete) and it is likely to contain material that is lost as fine sediment. In addition, being purely erosive and relatively hard, it will have a different equilibrium profile to that of the beach and will take longer to achieve equilibrium (FMI 2008).

Relatively little work has been done on the relationship between sea-level rise and the profiles of composite beach/rock, sandstone/siltstone shores. Recent results indicate that such profiles do change, becoming steeper as the rate of sea level rise increases (Walkden and Hall 2005).

Figure 27. Cape Elizabeth shoreline, north of Taholah (Workman 2012).

Figure 28. Quinault Formation of the QIR ocean shoreline north of Cape Elizabeth (Workman 2012).

Shore wave heights are normally limited by water depth, so an increase in sea level might be expected to increase wave height at the shore. This appears to be true at composite beach-rock shores, however it does not necessarily occur this way at all beach shores. The impact near Taholah, at the Quinault River, will likely see increases to the sedimentation retained at the mouth of the Quinault River to the ocean. The accumulation of heavy, coarse woody debris along the shoreline, and the wave activity to the shoreline because of up-shore and down-shore wave interactions will most likely increase the retention of this large woody debris along this shoreline. Slightly further south to Wreck Creek, south of Point Grenville, the river ocean interface will conceptually witness increases to wave height and force, resulting in scouring of the mouth of Wreck Creek to create onshore, intertidal estuaries.

Figure 29. Duck Creek Diapir formation (piercement structure) is composed of deep-sea sediments that were squeezed up though a fault in the sandstone cap (Workman 2012).

4.1. Coastline Response to Changed Storm Patterns

Shoreline structure depends strongly on the wave energy it is exposed to. Larger waves erode both the beach materials and the base of shoreline cliff structures (Boon 2007). The angle at which waves arrive to the shore has a strong effect on the rate at which beach material is redistributed along the shore and where it is transported to. A shoreline may represent a dynamic balance between the wave climate, land erosion, and the distribution of beach sediment. Changes to the wave climate, such as a shift in average direction or a general increase in wave height, will disturb this balance, and a period of shoreline adjustment is expected (FMI 2008).

These phenomena were seen along North American coastlines after the 2011 tsunami in Japan. The immediate force of the Japanese Subduction zone earthquake sent energy surges through the oceans to the distant shorelines. These created temporary changes to the wave climate along the QIR marine shorelines. Large woody debris stockpiled along the shorelines were redistributed up and down the coastline in response to the energy disbursement initiated along the Japan coastlines. In time, the “normal” wave patterns returned and large woody debris distribution was reestablished.

It is generally accepted that climate change leading to increasing ocean levels, changes to global weather patterns, and the distribution of precipitation as rain instead of snow, will bring noteworthy adjustments to the impacts of natural processes on the QIR marine coastlines. Direct predictions lead to concern for the long-term durability of coastal communities because of the sea-level elevation changes, the immediate closeness to the ocean shoreline, and the mélange of parent materials that include both river and ocean deposited sediments, coarse woody materials, unconsolidated river and glacial gravels, peat, piercement structures, and isolated erosion resistant outcroppings (like basalt).

4.2. Estimates for the Future

The climatological patterns of the world have cycled through several periods of extremely low global temperature regimes, and very hot cycles (Figure 16). The current millennia show the planet leaving the lowest of the temperature cycles progressing in the direction of global warming. On a global scale, it is widely accepted within the scientific community that global climate change is real.

One important subject to consider, is to what extent human generated atmospheric emissions have been increasing the rate of global climate change, or if they are inconsequential to the current global warming cycle.

Relative sea level rise is the result of several factors, including: the thermal expansion of ocean waters, vertical land deformation (e.g., tectonic movements), and melting glaciers and ice fields (Glick, Clough and Nunley 2007), as well as seasonal water surface elevation changes due to local atmospheric circulation effects (Mote, et al. 2008).

Thermal expansion of seawater is witnessed when seawater expands as it is warmed. The source of this added oceanic warmth is increased global atmospheric temperatures. Rising global temperatures are largely attributable to increased carbon emissions into the Earth’s atmosphere. Anthropogenic influences are responsible for the majority of current atmospheric carbon emissions (IPCC 2007). The thermal expansion of seawater accounts for approximately one-half of the global projected sea level rise in the 21st century (Mote, et al. 2008).

Several potential effects can be estimated for the QIR marine coastlines with the impacts expected to be realized progressively over the coming century. These changes are expected to be realized relatively slowly (Table 4).

Table 4. Hypothesized effects of climate alterations on marine shorelines and coastal estuaries (Ruggiero, et al. 2011).

Climate Alteration	Potential Effects
Extreme RSLC Increase	Increased inundation of estuarine habitats including tidal flats, marshes, and submerged aquatic vegetation, especially along moderately sloped shorelines.
Increased intrusion of oceanic water into estuaries.	Extent of effect will vary with relative river flow rate, location in the estuary, and RSLC rise rates in the vicinity of the estuary.
Increased winter precipitation and decreased summer precipitation	Increased winter–early spring flow of coastal rivers and creeks and reduced flow during summer. Extent of effect related to relative river flow, with a greater impact on river-dominated estuaries (e.g., Quinault) and tidal coastal creeks (e.g., Duck Creek and Raft River) than on tide-dominated estuaries (e.g., Moclips River), with smallest effect on bar-built estuaries (e.g., Queets).
Increased snow melt	Change in seasonal pattern of river flow into the Queets and Quinault Rivers; minor changes in other coastal estuaries and creeks.
Increased air temperature	Potential vulnerability of intertidal organisms because of the intertidal area in Quinault Marine Shoreline estuaries that may be exposed to elevated temperatures. Air temperature also has the potential to influence water temperatures particularly in the upriver portions of estuaries.
Increased offshore upwelling currents	Increased advection of high nutrient ocean water into lower estuaries during summer. Possible increase in the advection of low dissolved oxygen and low pH water into lower estuaries during the summer. Changes associated with upwelling may be more important in tidal influenced, versus river, dominated estuary reaches.
Increased storm activity	Potential scouring of shorelines and redistribution of protective large woody debris, adjacent to river outlets where marine shorelines are not protected by reefs or jetties to break apart the forces of high energy storm fronts.
Ocean acidification	Unknown effect on estuaries or how alterations may vary across estuary classes. Key marine organisms, such as mollusks, corals, and some plankton, will have difficulty maintaining their external calcium carbonate shells as ocean acidification increases.

4.3. Projections for Relative Sea Level Change

This analysis considers a range of IPCC sea-level rise scenarios, from a 0.08 meter (3.0 inch) rise in global average sea level by 2025 to a 0.69 meter (27.3 inch) rise by 2100. Results for this study are based on relative sea-level change for the QIR, taking into consideration land elevation changes due to geological factors, such as isostatic rebound, and ecological factors such as the impacts of the Columbia River Littoral Zone.

The IPCC estimated global sea level rise in 2007 giving attention to anthropogenic impacts of fossil fuel emissions and global climate change, and the accelerated speed of melting of the Greenland ice sheet and warming of Antarctica. The overall anthropogenic contribution to climate change has become better understood.

According to the IPCC, the factors of thermal expansion, geologic movement, and melting glaciers and ice fields contributed approximately 3.1 mm (±0.7 mm) of sea level rise globally per year between 1993 and 2003 (IPCC 2007). Estimates of future global sea level rise are primarily determined through tidal gauge records and considered with either numeric models or actual measurements of the Earth’s tectonic movement. The long-term projections for sea level rise are given as ranges. These estimates incorporate such a multitude of factors that, given a sudden, dramatic change in any of the variables (such as a CSZ earthquake and Juan de Fuca Plate adjustment), the extreme estimate (on either end of the spectrum) may become more accurate.

The IPCC estimate is that the global sea level rise through 2100 (independent of geologic factors locally), will increase at a rate of approximately 3.4 mm per year in the moderate scenario, with 1.8 mm in the low estimate and 5.9 mm in the high estimate (Table 5). These estimates project relative changes from sea level increases of 7.1”, 13.4”, or 23.2” by 2100 (provided as low, intermediate, or high estimates, respectively) (IPCC 2007).

The Quinault Marine coastlines experience isostatic rebound effects of approximately 1.2 mm per year in most cases, except notably at Kalaloch where a syncline has been identified to show a sinkhole where RSLC impacts will be greater. Within the 3 scenario projected by the IPCC, the Quinault Marine Shorelines will most likely see RSLC from 0.6 mm/yr to 4.7 mm/yr over the coming century (Table 5).

Table 5. Relative Sea Level Changes for Quinault Marine Coastlines through 2100.

Estimates for RSLC through 2100 in 3 scenario	IPCC estimated Global Annual Sea Level Rise	Quinault’s Estimated Annual Geostatc Rebound	Annual Relative Sea Level Change	Relative Sea Level Change 2100
Low	1.8034 mm	1.2 mm	0.60 mm/yr	53 mm (2.10”)
Intermediate	3.4036 mm	1.2 mm	2.20 mm/yr	194 mm (7.63”)
High	5.8928 mm	1.2 mm	4.69 mm/yr	413 mm (16.26”)
	Seawater Elevation Increases	Land Rebounds (rises)	All Scenario have an increase in RSLC	

Subsequent studies have explored the viability of different emission scenario globally to verify “low” and “high” greenhouse gas emission levels, as did the IPCC. All of these efforts have resulted in changed projections to the future greenhouse gas emission rates and resulting changes to the global sea level rise estimates.

There are additional local factors that influence sea levels. These include: oceanic winds, coastal winds, and local atmospheric pressure patterns. Another local factor in assessing sea level rise is inter-annual sea level variability, including the meteorological impacts associated with El Niño. In Washington, northward-driven winds along the outer coast (which are common in winter) combine with the Earth’s rotation to push ocean water toward the shore, elevating sea levels regionally (Mote, et al. 2008, Mass 2008). In El Niño years, this effect on sea level is intensified. This has resulted in average winter sea levels that are 20 – 32” higher than in the summer, for a duration of several months (Mote, et al. 2008).

Global climate change also has the potential to increase the intensity of storms and weather systems; considering this, the wintertime northward winds could increase in strength over future decades. However, it is important to note that the intensity of storms does not always equate to increased precipitation levels; Mote (2008) states that the human influence on precipitation is less predictable than the human influence on temperatures and that there is little indication that precipitation in the 21st century will vary significantly from precipitation in the 20th century.

Changes in wave action, as a result of meteorological changes, must also be considered in estimating and planning for future sea level rise. Heightened wave setup, a physical process by which wave energy raises the mean level of the sea, can increase extreme wave heights. Because this effect is dependent on large open-ocean-derived waves, average sea levels during storm events would only likely increase where swell is present (swell is the result of large waves produced in the open ocean). The potential for this increase in wave heights could be particularly hazardous in areas where increased sea levels are impacting human development and aquatic habitats (such as near Taholah and along the Grenville Bay areas).

4.4. Planning for Relative Sea Level Changes

Considerations for increased sea levels along the Quinault marine coastline give concern to marine habitat impacts, human habitation, and infrastructure support. The anticipated changes over the coming century are not likely to be realized consistently. Their comprehension will most likely come in surges as a road is washed out, a home structure is flooded, or landslides along a cliff shoreline undercut by ocean waves causes damages to the features on top of the cliff.

4.4.1. Marine Habitat

Marine habitat impacts are at risk to the loss of estuarine beaches, tidal flats, inland and tidal fresh marshes and swamps, and brackish marshes (Glick, Clough and Nunley 2007). These ocean influenced habitats will face several changes to structure, salinity, temperature, nutrient cycling, pH levels, and sedimentation. Those factors of habitat management are beyond the scope of this planning effort, but must be understood by resource managers to comprehend the changes anticipated in these near-shore environments.

4.4.2. Human Habitation

The potential impacts for human habitation are anticipated in 1) Taholah, 2) along SR109 south of Swede Hill along Grenville Bay, and to a lesser degree 3) in Queets. The reduced concern for Queets is because of the higher elevation of this community, the distance from the village to the marine shoreline, and the isostatic rebound of this area seen in response to the syncline lowering of Kalaloch and anticipated uplift in Queets in response to the syncline.

The RSLC concerns for Taholah are accompanied by the population density of this area combined with the risk profile of this village for tsunami threat (Schlosser 2010). Increased peak river flow levels along the Quinault River are anticipated from larger wintertime flow rates, reduced snow and ice sequestration in the Mount Anderson glacier complex, and general warming of the climate. The predicted weather pattern adjustments show reduced summer precipitation but increased winter precipitation leading to more rain on saturated soils, which will lead to increased river flow rates in winter.

Scouring from the increased flow rates in the Quinault River, will be seen near Taholah as increased sediment deposition and increased pressures for river meandering. As the Quinault River enters the Pacific Ocean the gradual RSLC lift at the mouth of the river will most likely be offset by a wearing down of the juncture and natural estuary development processes. These estuary formation pressures will include the result of pressures on human habitation structures and infrastructure, especially south of the Quinault River. These pressures will be realized slowly over the coming century.

4.4.3. Infrastructure Support

The effects of RSLC on coastally juxtaposed infrastructure projects, particularly to low-lying coastal developments may raise particular concern. Immediately, the challenges for SR109 south of Swede Hill and along Grenville Bay, present concerns to tidal inundation during storm events initially, and from RSLC within the coming century. The reach of the highway is a primary access route for Tribal business and the Continuity of Operations for the Quinault Indian Nation (Schlosser 2011). The increase of RSLC by only a small amount when coupled with warming ocean waters and increased storm energy events can overtop the highway and weaken it beyond use. An alternative access route (such as the McBride-Aloha Mainline Route (Schlosser

2010)) should be identified and fulfilled before planning and preparation efforts are sacrificed for the need to instantly implement a solution.

A related infrastructure concern is the roads near the cliff shorelines used for forestry and parcel access. These roads can be devastated or compromised by stream crossing failures (bridges) and by road material erosion where cliff lines retreat from the shoreline. Many road segments have already faced this compromise, especially where timber harvesting along the margin of the cliffs has sped erosion forces.

Chapter 5. Works Cited

ArchitectJaved.com. "Inspired Architecture." *Earthquakes.* 2012. http://articles.architectjaved.com/earthquake-geophysics/files/2010/09/asthenosphere.jpg (accessed 11 28, 2012).

Atwater, B.F., S. Musumi-Rokkaku, S. Kenji, T. Yoshinobu, U. Kazue, and D.K. Yamaguchi. *The Orphan Tsunami of 1700, United States Geological Survey.* Reston, Virginia, University of Washington Press: U.S. Geological Survey Professional Paper 1707, 2005.

Auster, P.J., and R.W. Langton. "The effects of fishing on fish habitat." *Fish Habitat: Essential Fish Habitat and Rehabilitation. American Fisheries Society*, 1999: 150-187.

Bolin, B., E.T. Degens, S. Kempe, and P. Ketner. *The Global Carbon Cycle.* Vol. SCOPE report 13. John Wiley & Sons, 1977.

Boon, J. "Ernesto: Anatomy of a Storm Tide." *Virginia Institute of Marine Science, College of William and Mary.* 2007. http://www.vims.edu/physical/research/ernesto.pdf (accessed November 11, 2010).

Burke Museum. "The Burke Museum of Natural History and Culture." *Cascade Episode.* 2012. http://www.burkemuseum.org/static/geo_history_wa/Cascade%20Episode.htm (accessed August 1, 2012).

Burton, I. *Vulnerability and adaptive change in the context of climate and climate change.* Climatic Change 36, The Netherlands, : Kluwer Academic Publications, 1997, 185-196.

Crandell, D.R. "Pleistocene glaciations of the southwestern Olympic Peninsula, Washington, USA." Geological Survey Professional Paper (501-B), 1964, 135-139.

Crandell, D.R. *The Glacial History of Western Washington and Oregon.* The Quaternary of the United States, Princeton University Press, 1965, 341-353.

CREW. "Cascadia Region Earthquake Workgroup." *Cascadia Subduction Zone Earthquakes: A Magnitude 9.0 earthquake scenario.* 2005. www.CREW.org (accessed August 2009).

Crystal, E. "Woolly Mammoths - Mammuthus primigenius." *Crystal Links.* 2010. http://www.crystalinks.com/woollymammoth.html (accessed June 10, 2012).

Davis, J. "Hazards of Sea Level Rise: An Introduction." *Harvard-Smithsonian Center for Astrophysics; Space Geodesy Group.* 2005. http://www.cfa.harvard.edu/space_geodesy/SEALEVEL/ (accessed August 2, 2012).

Dayton, P.K. "Competition, disturbance and community organization: the provision and subsequent utilization of space in a rocky intertidal community." *Ecological Monographs*, 1971: 41(4):351-389.

Dore, J.E., R. Lukas, D.W. Sadler, M.J. Church, and D.M. Karl. "Physical and biogeochemical modulation of ocean acidification in the central North Pacific." *Proceedings of National Academy of Sciences of the United States of America*, 2009: Rep., 12235-12240 pp.

Eaton, D.W., and A. Fredricksen. "Seismic evidence for convection-driven motion of the North American plate." *Nature*, 2007: 446, 428-431 .

Feely, R.A., C.L. Sabine, J.M. Hernandez-Ayon, D. Ianson, and B. Hales. "Evidence for Upwelling of Corrosive "Acidified" Water onto the Continental Shelf." *Science*, 2008: Vol. 320 no. 5882 pp. 1490-1492.

Feely, R.A., et al. "Impact of anthropogenic CO2 on the CaCO3 system in the oceans." *Science*, 2004: 305(362-366).

FMI. "The COASTAL PORTHOLE; the effects on climate change on coastline evolution." *Flanders Marine Institute.* 2008. http://www.coastalwiki.org/coastalwiki/Effect_of_climate_change_on_coastline_evolution (accessed March 15, 2012).

Gelfenbaum, G., et al. "THE COLUMBIA RIVER LITTORAL CELL: A SEDIMENT BUDGET OVERVIEW." *Coastal Sediments '99 Proceedings of the 4th International Conference on Coastal Engineering and Coastal Sediment Processes.* American Society of Civil Engineers: Long Island, NY, 1999.

Geller, D. *Cascadia Subduction Zone Volcanism in British Columbia.* Emporia, Kansas.: Emporia State University, 2008.

Glick, P., J. Clough, and B. Nunley. *Sea-level Rise and Coastal Habitats in the Pacific Northwest: An Analysis for Puget Sound, Southwestern Washington, and Northwestern Oregon.* Prepared for the National Wildlife Federation., 2007.

Gooding, R. "Starfish defy climate change gloom." *NewScientist (issue 2710)*, 2009.

Grove, T.L., N. Chatterjee, S.W. Parman, and E. Médard. "The Influence of H2O on Mantle Wedge Melting." *Earth and Planetary Science Letters*, 2006: 249, 74-89.

Hellwig, J.L. "The Interaction of Climate, Tectonics, and Topography in the Olympic Mountains of Washington State." Masters Thesis, Department of Geology, University of Illinois, Urbana, 2010, 355.

Holdahl, S.R., F. Faucher, and H. Dragert. "Contemporary vertical crustal motion in the Pacific Northwest." Edited by Choen and Vanicek. *American Geophysical Union, Geophysical Monograph* Slow deformation and transmission of stress in the earth (1989): 49.

Houghton, J.T., L.G. Meira Filho, B.A. Callander, N. Harris, A. Kattenberg, and K. Maskel. *Intergovernmental Panel on Climate Change 1995.* Vol. The Science of Climate Change. Cambridge, UK: Cambridge University Press, 1995.

Hyndman, R.D., E.E. Davis, and J.A. Wright. "The Measurement of Marine Geothermal Heat Flow by a Multipenetration Probe with Digital Acoustic Telemetry and in situ Conductivity." *Marine Geophys. Res. 4*, 1979: 181-205.

Hyndman, R.D., et al. *Giant earthquakes beneath Canada's West coast.* January 15, 2008. http://www.nrcan.gc.ca/earth-sciences/energy-mineral/geology/geodynamics/earthquake-processes/ (accessed July 6, 2012).

IPCC. *Summary for Policymakers. In: Climate Change 2007: The Physical Science Basis.* Contribution of Working Group I to the Fourth Assessment Report of the Intergovernmental Panel on Climate Change [Solomon, S., D. Qin, M. Manning, Z. Chen, M. Marquis, K.B. Averyt, M. Tignor and H.L. Miller (eds.)]., Cambridge: Cambridge University Press, 2007.

Jacoby, G.C., D.E. Bunker, and B.E. Benson. "Tree-Ring evidence for an A.D. 1700 Cascadia earthquake in Washington and northern Oregon." *Geology*, 1997: 25(11): 999-1002.

Kious, W.J., and R.I. Tilling. "Plate tectonics and people." *USGS.* May 5, 1999. http://pubs.usgs.gov/publications/text/tectonics.html (accessed June 10, 2012).

Kirby, S., K. Wang, and S. Dunlop. "The Cascadia Subduction Zone and Related Subduction Systems." Open File Report 02-328, USGS, 2002.

Kurihara, H. "Effects of CO2-driven ocean acidification on the early developmental stages of invertebrates." *Marine Ecology Progress Series*, 2008: 373, 275-284.

Leonard, L.J., R.D. Hyndman, and S. Mazzotti. "Coseismic subsidence in the 1700 great Cascadia earthquake: Coastal estimates versus elastic dislocation models." GSA Bulletin 116: 655-670, doi: 10.1130/ B25369.1, 2004.

Levi-Setti, Riccardo. *Triblobites.* Chicago: University of Chicago Press, 1995.

Margaritondo, G. "Explaining the physics of tsunamis to undergraduate and non-physics students." *European Journal of Physics*, 2005: 26.

Mass, C. *The Weather of the Pacific Northwest.* Seattle: University of Washington Press, 2008.

McCroy, P.A., D.S. Foster, W.W. Danforth, and M.R. Hamer. "Crustal deformation at the leading edge of the Oregon Coast Range block, Offshore Washington (Columbia River to Hoh River); Crustal-block motions complicate the slip rates of seismotectonic elements of the Cascadia subduction boundary." USGS Professional Paper 1661-A, 2002, 53.

Mills, L.S., M.E. Soule, and D.F. Doak. "The Keystone-Species Concept in Ecology and Conservation." *BioScience*, 1993: 43 (4), 219.

Mote, P., A. Petersen, S. Reeder, H. Shipman, and L. Whitely-Binder. *Sea Level Rise in the Coastal Waters of Washington State.* Seattle: A report by the University of Washington Climate Impacts Group and the Washington Department of Ecology, 2008.

NGDC. *Tsunami Events Full Search. National Geophysical Data Center, National Oceanic and Atmospheric Administration Satellite and Information Service.* 2010. http://www.ngdc.noaa.gov/ (accessed February 26, 2010).

NOAA. "National Weather Service Forecast Office." *Elko, Nevada.* 2011. http://www.wrh.noaa.gov/lkn/photogal.php (accessed May 14, 2011).

Norse, E. "Global marine biological diversity: a strategy for building conservation into decision making." *Center for Marine Conservation* (Island Press), 1994: 383.

NPS. "History & Culture." *United States Park Service.* 2009. http://www.nps.gov/olym/historyculture/index.htm (accessed July 6, 2012).

NRC. "Natural Resources Canada." *Cascadia Subduction Zone.* January 15, 2008. http://www.nrcan.gc.ca/earth-sciences/energy-mineral/geology/geodynamics/earthquake-processes/9141 (accessed August 11, 2012).

NRCS Soil Survey Staff. *Soil taxonomy: A basic system of soil classification for making and interpreting soil surveys. 2nd edition.* U.S. Department of Agriculture Handbook, Natural Resources Conservation Service, 1999, 436.

Olympic Coast National Marine Sanctuary. "Final Management Plan and Environmental Assessment." NEPA EA, Olympic Coast National Marine Sanctuary, NOAA, Port Angeles, 2011, 352.

Orange, D.L., and K.A. Campbell. "Where Continental and Oceanic Plates Collide." *Quinault Natural Resources*, Spring/Summer 1996: 36-47.

Orghidan, T. "Ein neuer Lebensraum des unterirdischen Wassers: Der hyporheische Biotop." *Archiv für Hydrobilogie.* Stuttgart, Germany: Schweizerbart, 1959. 55:392–414.

Orr, J.C., et al. "Anthropogenic ocean acidification over the twenty-first century and its impact on calcifying organisms." *Nature* 437 (2005): 681-686.

Patsch, K, and G. Griggs. *Littoral Cells, Sand Budgets, and Beaches.* Santa Cruz: INSTITUTE OF MARINE SCIENCES, 2006.

Pazzaglia, F.J., and M.T. Brandon. "A Fluvial Record of Long-Term Steady-State Uplift and Erosion Across the Cascadia Forearc High, Western Washington State." *American Journal of Science* 301 (2001): 385-431.

Phipps, J.B. *Coastal Accretion and Erosion in Washington State 1977-1987; Shorelands and Coastal Zone Management Program.* Olympia, Washington: Washington Department of Ecology, 1990, 33 pp.

PRISM Climate Group. *PRISM Climate Group.* Edited by Dr. Christopher Daly. Oregon State University. June 10, 2012. http://prism.oregonstate.edu (accessed July 1, 2012).

Rau, W.W. "Geology of the Washington Coast; Point Grenville and the Hoh River." Washington Department of Natural Resources; Geology and Earth Resources Division., Olympia, 1973.

Rigg, G.B., and R.C. Miller. "Intertidal plant and animal zonation in the vicinity of Neah Bay, Washington." *Proceedings of the California Academy of Sciences, San Francisco*, 1949: 26(10):323-351.

Ruggiero, P., C.A. Brown, P.D. Komar, J.C. Allan, D.A. Reusser, and H. Lee. "Impacts of climate change on Oregon's coasts and estuaries." *Department of Geosciences, Oregon State University*, April 8, 2011: 211-268.

Schaefer, M.B. *The Present Status of the Razor Clam Stocks in the State of Washington.* Olympia: Washington Department of Fisheries, 1939.

Schalk, R. *The Evolution and Diversification of Native Land Use Systems on the Olympic Peninsula.* Seattle: University of Washington, 1988.

Schalk, R., and D. Yesner. "THE REGIONAL ENVIRONMENT AND FOOD RESOURCES OF THE OLYMPIC PENINSULA." In *The Evolution and Diversification of Native Land Use Systems on the Olympic Peninsula*, by R. Schalk. Seattle: University of Washington, 1988.

Schlosser, W.E. *Quinault Indian Nation Comprehensive Emergency Operations Plan.* Pullman, WA: Kamiak Ridge, LLC, 2011.

Schlosser, W.E. *Quinault Indian Reservation Tribal Hazard Mitigation Plan.* FEMA Tribal Hazards Mitigation Plan, Pullman, WA: Kamiak Ridge, LLC, 2010, 396.

Schlosser, W.E., J.H. Bassman, F.G. Wagner, and P.R. Wandschneider. "Increasing long-term storage of carbon sequestered in Russian softwood logs through enhanced lumber recovery." *Forest Products Journal*, 2002: 26.

Schlosser, W.E., J.H. Bassman, P.R. Wandschneider, and R.L. Everett. "A carbon balance assessment for containerized Larix gmelinii seedlings in the Russian Far East." *Forest Ecology and Management* Volume 173, Issues 1–3 (2003): 335-351.

Schlosser, W.E., W.E. Armstrong, and B.R Schlosser. *Upper Quinault River Salmon Habitat Restoration NEPA Compliance.* NEPA COmplicance EA, Pullman, WA: Kamiak Ridge, LLC, 2011, 247.

Scotese, C.R. "PALEOMAR Project." *PALEOMAP.* 2002. http://www.scotese.com (accessed April 21, 2012).

Speicer, R.C. *Glaciers in the Olympic Mountains, Washington: Present Distribution and Recent Variations.* Masters Thesis, Seattle: University of Washington, 1986, 158.

Spicer, R. C. "Recent Variations of Blue Glacier, Olympic Mountains, Washington, U.S.A." *Arctic and Alpine Research, Vol. 21, No. 1*, 1989: 1-21.

Thackray, G.D. "Convergent-margin deformation of Pleistocene strata on the Olympic coast of Washington, USA." *The Geological Society*, 1999: 199-211.

Thackray, G.D. "Extensive Early and Middle Wisconsin Glaciation on the Western Olympic Peninsula, Washington, and the Variability of Pacific Moisture Delivery to the Northwestern United States." *Quaternary Research* 55 (2001): 257-270.

Thackray, G.D. "Glaciation and coastal neotectonic deformation on the western Olympic Peninsula, Washington." Friends of the Plistocene, 1996.

Thorson, R.M. "Ice-Sheet Glaciation of the Puget Lowland, Washington during the Vashon Stade (Late Pleistocene)." *Quaternary Research* 13 (1980): 303-321.

Thrush, S.F., and P.K. Dayton. "Disturbance to marine benthic habitats by trawling and dredging: implications for marine biodiversity." *Annual Review of Ecology and Systematics 33*, 2002: 449-479.

USGS. "Maps." *Southwest Washington Coastal Erosion Study.* March 22, 2012. http://www.ecy.wa.gov/programs/sea/swces/products/maps.htm (accessed May 5, 2012).

—. "US Geological Survey." *Local Tsunamis in the Pacific Northwest.* 2010. http://earthquake.usgs.gov/regional/pacnw/paleo/greateq/index.php (accessed February 27, 2010).

—. "US Geological Survey." 2009. http://earthquake.usgs.gov/regional/pacnw/paleo/greateq/index.php.

UW. *Tsunami!* 2012. http://www.ess.washington.edu/tsunami/index.html (accessed September 9, 2012).

Verdonck, D. "Contemporary vertical crustal deformation in Cascadia." *Technophysics*, 2006: 417: 221–230.

Vygodskaya, N.N., et al. "Leaf conductance and CO2 assimilation of Larix gmelinii growing in eastern Siberian boreal forest." *Tree Physiol*, 1997: 607-615.

WaDNR. "Washington Department of Natural Resources." *Earthquakes in Washington.* 2010. http://www.dnr.wa.gov/ResearchScience/Topics/GeologicHazardsMapping/Pages/earthquakes.aspx (accessed February 24, 2010).

Walkden, M.J., and J.W. Hall. "A predictive mesoscale model of the erosion and profile development of soft rock shores." *Coast Engineering*, 2005: 52, 535–563.

Wessen, G.C. *An archaeological survey of the proposed Coast Guard Stations at La Push, Washington.* Washington Archaeological Research Center Project report No. 69, Pullman: Washington State University, 1977.

Williams, H. *The Restless Northwest; A Geologic Story.* Pullman: Washington State University, 2002.

Wood, C.A., and J. Kienle. *Volcanoes of North America: United States and Canada.* Cambridge University Press, 354p., p.149, 1990.

Wood, N., and C. Soulard. "Variations in Community Exposure and Sensitivity to Tsunami Hazards on the Open-Ocean and Strait of Juan de Fuca Coasts of Washington." *U.S. Geological Survey.* 2008. http://pubs.usgs.gov/sir/2008/5004/ (accessed 2010).

Workman, L.J. *Photography taken by Larry Workman on the QIR and provided for use in this planning effort. Reproduced with permission.* Quinault Indian Nation, Taholah.

Workman, L.J. *The Land of Trees; Scannings from Quinault Country, the Grays Harbor Region, and Beyond 1774-2010.* Updated report, Taholah: Quinault Indian Nation, 2010.

WSMD. *Washington State Military Department (WSMD) Hazard Identification and Vulnerability Assessment (HIVA).* Emergency Management Division, Olympia: An Assessment of Hazards and Risks to the People, Economy, Environment, and Property of Washington State, 2009.

Citation of this work:

Schlosser, W.E. 2013. Relative Sea Level Change Along Quinault Indian Reservation Marine Coastlines . Kamiak Ridge, LLC, Pullman, WA, January 31, 2013. Pp 58.

Last Page of Report

Remainder Intentionally Left Blank